THE UNIVERSITY OF QUEENSLAND

Design of Hydraulic Bottom-Out Control for Mountain Bike Suspension

Student Name: Ben BRUNCKHORST

Course Code: MECH4501

Supervisor: Professor Paul Meehan

Submission date: 1 June 2018

Faculty of Engineering, Architecture and Information Technology

Abstract

Engagement with downhill mountain bike engineers revealed a key opportunity to improve mountain bike suspension fork design by addressing 'bottom-out" from harsh impacts. Bottom-out causes damage to components, poor control and discomfort to the rider. This design thesis encompasses simulation, design, manufacture and testing of an adjustable bottom-out damper. The device increases damping forces in the final stage of compression. Simulation of the design demonstrates advantages over existing means to prevent bottom-out since greater control over the response is possible with fewer performance trade-offs. The prototype damper was designed and built from existing suspension componentry and custom manufactured parts to integrate with an existing suspension fork. The prototype was validated by testing on a bicycle for a typical impact which yielded results in line with predictions. Specifically, the damper decreased compression amplitudes by up to 20% and settling time by 27%. Tyre contact with the ground was extended by 0.24 seconds for the given impact and variation in normal force was reduced by one third resulting in improved traction. This translates to a more controlled mountain bike, greater predictability for riders and potentially higher speeds in downhill mountain bike racing. The design was successful in controlling for bottom-out and improves mountain bike suspension performance. Further validation is warranted to consider future production of the design.

Acknowledgements

Many thanks must go to Nigel Reeve, of Canyon Factory Racing Team, who provided the initial inspiration for this project, guidance and access to the mountain bike industry.

I would like to thank Professor Paul Meehan for his supervision from vague initial idea to the completion of this thesis.

My heartfelt appreciation goes to my parents for their support and encouragement during this thesis, engineering degree and my life.

Finally, I can't thank my fiancée Rachael enough for her love and belief in me to complete this work, even when I was sure I had bitten off more than I could chew.

Table of Contents

List of Figures

List of Tables

1 Introduction

In recent years the world of downhill mountain bike racing has progressed with higher speeds becoming possible over rougher terrain. This has largely been driven by improved design of mountain bikes and their components. Perhaps of most significance, mountain bike suspension design has been refined to provide riders with more control and comfort. Many modern suspension units are coil or air sprung and have adjustable hydraulic damping in compression and rebound. High end bicycle suspension products borrow heavily from motocross and motorsport suspension but require lighter weight components and more precise tuning specific to particular terrain or rider.

Nowhere is the comparative performance of mountain bike suspension more evident than the *Union Cycliste Internationale* (UCI) downhill mountain bike World Cup series. Riders race against the clock while descending several hundred vertical metres over rough terrain for a duration of 2-5 minutes with top speeds up to 80 km/h. The World Cup is also an opportunity for the bicycle industry to test prototype designs and showcase their products. Engagement with industry has revealed a key opportunity to improve the design of mountain bike suspension forks by addressing problems associated with “bottoming” the suspension on harsh impacts. Bottoming, or completely compressing the suspension, has negative consequences including damage to components, poor suspension performance and injury to the rider. The need for increased damping at the end of the suspension stroke to prevent bottom-out is twofold. Firstly, to reduce impacts transmitted to the rider and frame and secondly to improve control and allow higher speeds over technical terrain. This should translate to a faster and more efficient ride, saving seconds on the racetrack.

1.1 Scope and Overview

This project encompasses simulation, design, prototype manufacture and testing of a bottom-out damper for a Rockshox Suspension Fork (figure 1). The device must be integrated to the suspension fork and not interfere with the existing suspension mechanisms. The component will provide an externally adjustable damping force at the end of the suspension stroke to address the bottom-out problem. The design will incorporate existing suspension components available to industry and custom manufactured parts working together as one system.

Figure 1: Rockshox Boxxer Fork (Rockshox, 2017)

This thesis begins with a review of relevant background and literature pertaining to bicycle suspension and damper design. Theory relevant to the design is then discussed. A simulation of mountain bike front suspension is developed from theory and used to compare potential solutions to the bottom-out problem to inform design. Following, the design process of a prototype damper and its manufacture is described in detail. Validation of the prototype damper using data acquisition from field testing is presented. A discussion of validation results draws a number of conclusions that could lead to production of the bottom-out damper and will inform the future development of mountain bike suspension.

1.2 Aims and Objectives

The project sets out to achieve the following aims:

- Design and manufacture an externally adjustable hydraulic bottom-out assembly (damper) for use in Rockshox suspension forks including:
    - proof of the concept through simulation; and,
    - test of the prototype to validate the design.
- Gain knowledge through a rapid design process working with the bicycle industry.
- Inform further development of mountain bike suspension technology.

The objectives of this design thesis are:

- to develop a realistic computer simulation for front bicycle suspension;
- to produce a detailed design;
- to manufacture a prototype model;
- to test the prototype and quantify its performance; and,
- to present findings, provide recommendations for improvement and identify opportunities for production.

To pursue these objectives, it is helpful to assume a detailed review of prior work relating to the design and analysis of vehicle suspension with emphasis on its application to mountain bikes.

2 Background

This chapter provides background information and research relevant to bicycle suspension design. Theory and literature specific to the evaluation and development of dampers is discussed in the context of mountain biking. Existing designs are considered with reference to the bottom-out problem in order to inform the proposed design project.

2.1 An Introduction to Bicycle Suspension

The quest to attenuate vehicle vibrations using a combination of spring and damper dates back to the beginning of automobile design. The first known suspension unit in this form was used by Renault at the 1906 French Grand Prix (Dixon 2007). A damper, introduced between the wheel mass and chassis mass generated forces by passing a piston through fluid. The telescoping suspension design we are familiar with today was developed soon after, originally for the design of aircraft landing gear. Much more recently, in the 1990s, suspension made its way onto bicycles designed specifically for off-road use. The design of suspension components for bicycles has largely drawn on knowledge of vehicle dynamics and control in general, with adaptations made for pedal powered use. This review provides background from which to commence design, an overview of literature evaluating suspension performance and an assessment of existing suspension designs to the bottom-out problem.

2.2 Bicycle Suspension in Theory

The front suspension on a mountain bike can be most simply modelled as a discrete system comprising of two masses, a spring and a damper shown in figure 2 and 3. Energy is transferred into the suspension either by the terrain displacing the wheel or by the rider shifting weight on the bicycle (Nielens & Lejeune 2004). The spring is an elastic element that stores potential energy when compressed. Both linear coil springs and progressive air springs are used for mountain bike suspension. The damper is typically a viscous element that dissipates energy. In the simplest of terms, the main function of suspension is to absorb energy. Hence, the design of the viscous element is an aspect that currently receives most attention in bicycle suspension design and is the subject of this project.

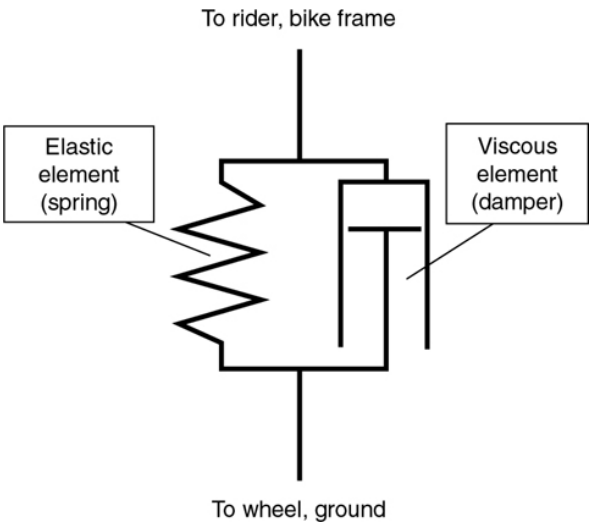

Figure 2: Spring-mass-damper model

Figure 3: Rockshox RS-1 Fork (Rockshox, 2017)

The sprung mass in our context is both the rider and bicycle above the suspension fork. The unsprung mass is the wheel, tyre and lower section of the fork. A smaller unsprung mass, with lower inertia, allows the suspension to react quickly in response to rapid changes in terrain (Croccolo & De Agostinis 2013). The ratio of the sprung mass to unsprung mass is lower on a bicycle than on other vehicles where components such as the engine add significantly to sprung mass. As a result, minimising the unsprung mass is particularly import in bicycle suspension design to improve its responsiveness to changes in terrain. The concept of reducing unsprung weight has recently driven the design of several “inverted” suspension forks that challenge traditional designs, such as the Rockshox RS-1 shown in figure 3 above.

2.3 Why Use Suspension for Mountain Biking?

The evaluation of mountain bike suspension systems and their performance attenuating vibrations has been the subject of several studies in recent years. Literature has predominately compared mechanical and physiological performance indicators for bicycles with and without suspension. It is widely supported that using suspension over rough terrain permits higher speeds for several reasons. Firstly, rougher terrain need not be avoided when suspension is used so straight-line velocity can be maintained and the centre of mass need not be displaced (Orendurff, Fujimoto & Smith 1994). Secondly, suspension improves traction by providing a more constant normal force than a rigid system, which also increases time the

tyre is in contact with the ground (MacRae et al. 2000). The normal force is proportional to the amount of friction between the tyre and ground. Hence, use of suspension translates to better braking performance, cornering and predictability of the bicycle. Thirdly, by absorbing energy, suspension can reduce the risk of injury due to impacts being transmitted through the bicycle (Macdermid 2015, 2017). This 'fatigue theory' exploring the increased comfort achieved when using suspension has been studied to the largest extent and is expanded below.

From a physiological perspective, researchers have examined the effect of vibrations on human performance across many contexts. For vibrations in general, Grether (1971) found that frequencies from 10-25 Hz can reduce sharpness of vision to an extent proportional to the vibration amplitude. Nakamura & Haverkamp (1991) find that vibrations do not affect fine motor control so long as amplitudes remain below 8 ms^{-2} in an experiment simulating vibrations on operators of earthmoving vehicles. More recently, a number of studies have attempted to quantify the effect of suspension on human performance while mountain biking.

Titlestad et al. (2003) studied the effect of suspension systems on physiological and psychological performance indicators by having participants ride on a test rig in both suspended and rigid configuration over simulated bumps. They recorded heart rate, oxygen consumption (VO2) and subjective measures of exertion and found them all to be lower on the suspended bicycle to a statistically significant level. Overwhelmingly, other literature supports that suspension reduces the amount of energy humans must otherwise expend to dissipate vibrations while riding. (Davie 2011). One study compared upper body muscle activity in cross country and downhill mountain biking and found it was strongly affected by the type of terrain. The downhill riders experienced a much higher level of muscle contraction, which indicates they were required to physically absorb more energy (Hurst et al. 2012). This highlights the importance of well performing suspension on downhill mountain bikes.

Macdermid (2015) contends that the high overall injury rate in mountain biking and in particular lower back, neck and wrist pain can be partly attributed to riders' exposure to complex vibrations varying in frequency, direction and amplitude. Additionally, experiments

have found that of the energy used by the rider to power the bicycle, the amount dissipated by suspension is negligible on most uneven terrain (Ishii et al. 2003). Since the pedalling efficiency trade-off is small, there is a very strong case that suspension improves overall off-road cycling performance. While suspension plays a beneficial role attenuating vibrations, it is importance to acknowledge that rider technique is also a significant determinant of impact exposure over the length of a mountain bike course with many obstacles (Miller et al. 2017).

From a mechanical perspective, Levy & Smith (2005) conducted an experiment that compared the vibration damping of 5 front suspension set ups on a mountain bike by quantifying accelerations at the axle and frame. They conducted a spectral analysis of input frequencies and identified low frequency vibrations in the range of 0-25 Hz are due to uneven terrain and therefore of primary concern for bike suspension. Those bikes with suspension forks reduced vibration amplitudes by 30-60% at the frame compared to the axle for this range of frequencies. Similar studies to quantify the performance of suspension fork models observe significantly lower vibrations transmitted from the axle to handlebars when the stiffness of fork is reduced (Orendurff, Fujimoto & Smith 1994, Laser & Bauer 1997). There remains no doubt suspension plays an important and significant role on mountain bikes.

The present body of literature specifically relating to the comparative performance of suspension designs is limited, with biomechanics and exercise physiology the main interest of the scientific community concerned with cycling. Nonetheless, these works are a helpful background to the operating conditions and performance objectives that should inform suspension design. They draw attention to the preliminary function of suspension to dissipate energy so that it is not transmitted to the rider. The following section focusses on design of the damping component that achieves this which is the primary subject of this project.

2.4 Damper Design

In a suspension system, a damper provides a resistive force proportional to velocity. This is typically achieved in a viscous damper by forcing fluid, commonly oil, through small passages when the suspension is in a dynamic state. Hence, the damper slows the compression or extension of a fork after a disturbance or impact. The proposed “hydraulic bottom-out

control” is a damper for the final stages of the suspension stroke to prevent full compression. Due to the harsh impacts that downhill bikes experience, it is not uncommon for suspension to reach full compression. When a mountain bike fork is fully compressed it acts the same as a rigid fork, offering no further impact absorption or energy dissipation. As a result, full compression events should be avoided to prevent negative consequences to bicycle and rider performance. Motorsport suspension addresses the bottom-out issue with a similar device to the proposed damper often referred to as a “hydraulic bump stop”, “bottoming cone” or “anti-bottoming device” (Bauer 2011). In dynamic conditions, a higher damping force reduces the likelihood of suspension reaching full compression. The damper will slow the rate of compression and thus reduce the total displacement of the suspension due to a harsh impact.

The damping force provided by a viscous damper at a particular velocity of depends on the viscosity of a fluid and restriction of the flow. The viscosity is determined by properties of the fluid, a more viscous oil may be used where higher damping. The restriction of the flow is determined by the geometry of the damper design as well as fluid properties and behaviour. Typically, in high performance suspension, a shim stack is used to control the flow of the fluid through the damper (Croccolo & De Agostinis 2013). A shim stack is a group of thin steel discs that obstruct oil ports and bend open due to pressure as the piston moves through fluid as shown in figure 4. The next section describes common damper components.

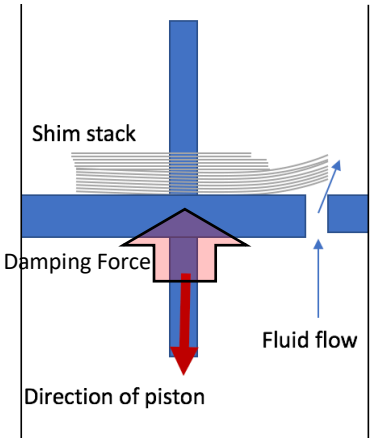

Figure 4: Damping with a shim stack

Higher damping forces may be achieved by using thicker shims that do not deflect as easily. The resultant ratio of damping force to velocity for a particular damper is defined as the damping coefficient (c) and has units Ns/m. Theoretical calculation of the damping coefficient is further discussed in the next chapter.

2.5 Damper components

The standard components of a typical vehicle suspension damper and their function are described below. A labelled diagram of two typical damper designs is shown in figure 5.

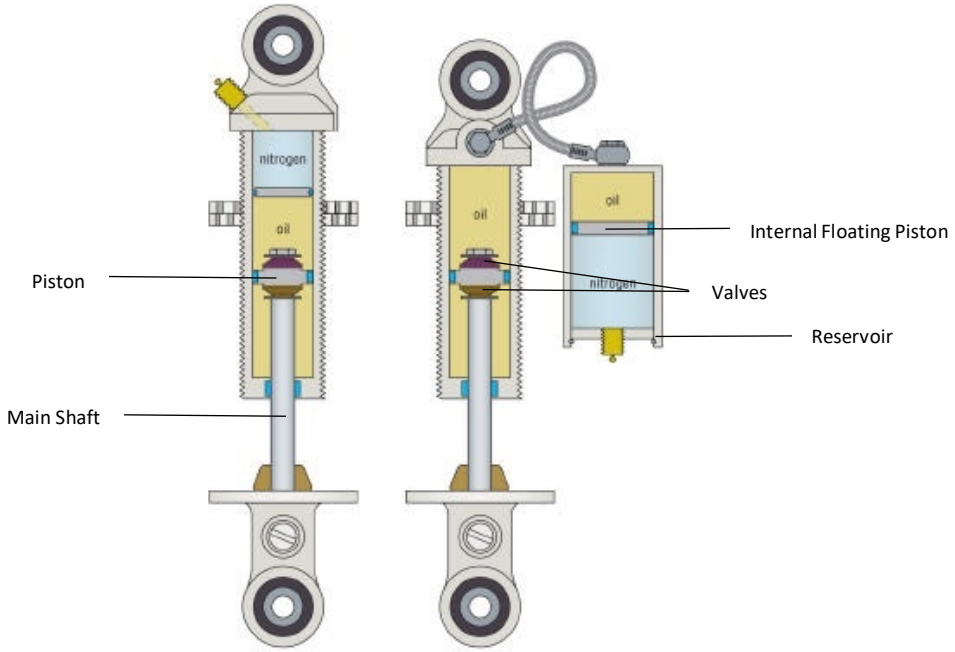

Figure 5: Monotube and external reservoir dampers (Racetech, 2018)

2.5.1 Body

The body of the damper contains the suspension fluid that is used to generate a damping force. It must provide a hydraulic seal to prevent fluid leaving the system and be able to withstand fluctuating internal fluid pressures when the suspension is in operation. The body also provides support for the shaft and piston, ensuring they can only displace in the direction of compression or extension. On a mountain bike fork, the damper body is usually a sealed cartridge located in one of the fork legs.

2.5.2 Main Shaft

The rod or main shaft couples the motion of the spring element to motion of the piston within the damper. The piston is attached at one end of the main shaft and moves axially through the damper when the spring compresses or extends. The main shaft experiences compression due to impacts and damping force so must be designed against buckling accordingly.

2.5.3 Piston

The piston divides the body into two sealed chambers and is attached to the end of the main shaft, as in figure 5. Small holes or oil ports allow oil to flow from one side to the other as the piston moves through the damper. The geometry of the piston will influence the damping characteristics of the system. Oil ports in the piston are usually covered by a valve in one flow direction, which allows independent control of the damping in both compression and extension.

2.5.4 Valve

The valve controls the flow of oil through the ports in the piston. Valves usually employ a shim stack to restrict fluid flow (see figure 4 above). These shims can take varying diameters and thickness which influenced the damping characteristics. The damping can also often be controlled using an external adjuster that changes the amount of preload on the shim stack.

2.5.5 Reservoir

An additional chamber in the damper, often called a reservoir, contains a gas such as nitrogen or air at high pressure to pressurise the damping fluid. The gas is separated from fluid by an internal floating piston which moves axially in the chamber depending on the compression of the suspension and resulting fluid pressure. Figure 5 shows an IFP within the damper body in one design and an external reservoir with an IFP in second design.

2.6 Emerging Damper Technology

When designing suspension, engineers traditionally face a trade-off between control and comfort. The suspension characteristics that enhance control cause less vibration isolation from the ground and are therefore less comfortable. More specifically, stiffer springs and higher damping forces enhance control whereas less stiff, less damped suspension provides greater comfort (Els et al. 2007). For competition downhill mountain bike racing, riders tend to run stiffer and slower (more damped) suspension in an effort to increase control rather than optimal comfort as race runs are short and time advantages depend more on bike handling. In a similar way Formula 1 suspension has very different requirements to passenger vehicle suspension. In mountain biking, manufacturers tend to produce suspension for the average rider with a balanced approach to this trade-off. As a result, there is scope to modify

suspension products on the market to better suit a racing application and this design project seizes the opportunity.

Recently, in an effort to reduce the trade-off between comfort and control engineers have explored new damper designs that can adapt to terrain, providing more of either comfort or control depending on conditions. In particular there has been the development of semi-active suspension, where damping and spring characteristics are electronically varied to best suit the terrain (Els et al. 2007). These systems often use variable magnetorheological (MR) or electrorheological (ER) dampers. In these dampers, the viscosity of the fluid is increased by the presence of a magnetic or electric field. Controllers use accelerometers on the vehicle to detect vibrations induced by the terrain and alter the viscosity of suspension oil to achieve a desirable damping force. Such designs are proven to improve suspension performance. Jiang & Wang (2012) compared a semi-active magnetorheological damper to a standard viscous damper for passenger vehicles and found that accelerations at the sprung mass were reduced by 15-24%. The use of MR fluids to control mountain bike suspension has also been investigated. Two experiments found an MR damper reduced vibrations for a bicycle fork compared to a conventional damper (Yeh & Chen 2013, Shiao & Nguyen 2015). However, these semiactive bicycle suspension designs compromise other aspects of performance by adding weight, cables and a power source, making them unfeasible for racing applications to date.

A more simplistic mechanical approach to adapting suspension characteristics to the conditions is position sensitive dampers. These provide higher damping forces, the further a spring is compressed. This may be achieved by using bypass valves that permit fluid to flow around the shim stack (or other flow constrictor) only for the beginning of the stroke. Position sensitive damping allows for better control under large impacts without reducing comfort when terrain induced vibrations are small. In doing so they provide more adaptive, better performing suspension similar to active suspension, though to a lesser extent. Currently position sensitive damping is not employed in mountain biking despite several approved patents for its use (Ericksen et al. 2012). Generally, this design represents added complexity and cost that manufacturers are not willing to embrace for the limited number of competitive

riders who would benefit. This project sets out to design a bottom-out damper that would introduce the concept of position sensitive damping to mountain biking.

2.7 Existing Methods of Bottom-Out Control

There are a number of approaches to addressing the bottom-out issue in mountain biking. Typically, the approach for bike suspension has focussed on increasing the spring stiffness for the elastic element in a suspension system. This has led to some innovative designs such as dual rate springs (Race Only Springs 2017), that have a higher stiffness only after a particular point in suspension travel is reached to prevent the fork bottoming out. Similarly, bottom-out bumpers made of rubber are often used to provide a softer stop by offering some compressibility when a fork reaches full compression. However, increasing the spring stiffness means that the elastic element can store more energy which must subsequently be dissipated by the damper. While it is an effective method reducing bottom-out consequences, increasing stiffness comes with a performance trade-off since more energy must be absorbed by the existing damper.

Hydraulic bottom-out systems have the advantage of adding another viscous damper element to the suspension that dissipates energy while also slowing the rate of compression to prevent bottom-out. They are effectively a second stage damper that causes damping of the system to be position sensitive. These designs are widely used in off-road motorcycle and rally car applications for better vehicle control under harsh impacts. These typically involve a piston that displaces oil through small bleed holes when it enters a tightly fitting socket near full compression as shown in figure 6. Size and weight constraints have meant limited application of hydraulic bottom-out control to mountain bike forks.

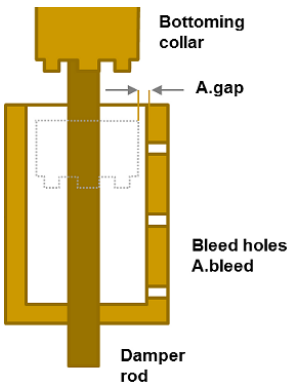

Figure 6: Hydraulic bottom-out (Croccolo & De Agostinis, 2013)

2.8 The Need for a Bottom-Out Damper

Mountain bike suspension plays a vital role to absorb impacts and dissipate energy. The harsh conditions encountered in downhill mountain bike racing are particularly demanding on suspension and engineers constantly face a delicate balance between comfort and control objectives in design. There is evidence that new technology can be applied in such a way that minimises this trade-off. Despite the demand for higher performance mountain bike suspension, at present none of the major manufacturers employ an adjustable hydraulic bottom-out device of any kind. This project set out to design a damper that fills that gap, improves suspension performance and can be added to an existing fork.

3 Theory for Design

This chapter outlines relevant theory to inform design of the bottom-out damper and development of a simulation. It considers dynamic models of the bike, damper and aspects of fluid theory relevant to design.

3.1 Dynamics of the bike

The front bike suspension can be modelled as a two degree of freedom system with both the front tyre and suspension acting as a mass-spring-damper as shown in figure 7. This model can be used to gain insight into how the suspension fork responds to ground disturbances.

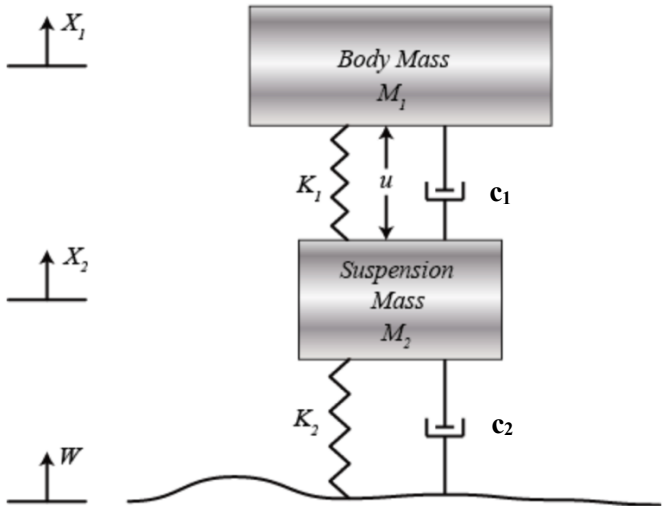

Figure 7: Half bike model

Downhill mountain bike tyres are inflated at relatively low air pressures (25 psi or 172 kPa). Consequently, the spring force (due to elastic response of compressed air) and damping (due to non-elastic response of rubber) are significant and should be included in the analysis. For this project, the main variable of interest is the displacement between the suspension mass and the body mass, or 'travel', and its derivatives with respect to time. This is physically equivalent to the visible portion of a mountain bike fork stanchion as shown in figure 8.

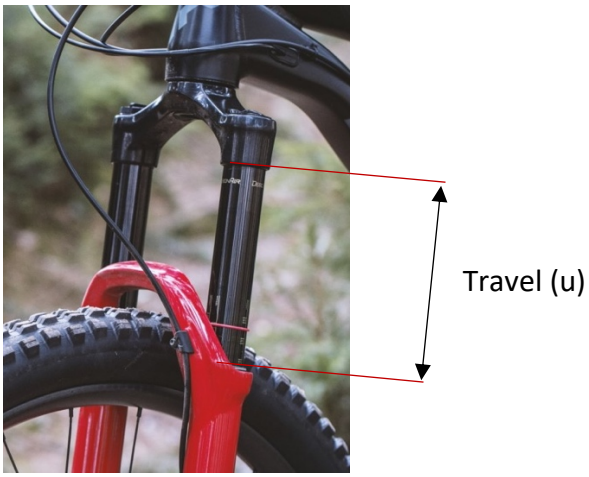

Figure 8: Bike front suspension travel

A model of the proposed bottom-out is shown below in figure 9, with a third damper that acts only when travel (u) approaches zero (full compression). When active, the two dampers between the body mass and suspension mass act in parallel and can be modelled as an equivalent damper (with damping coefficient given by c_1+c_3).

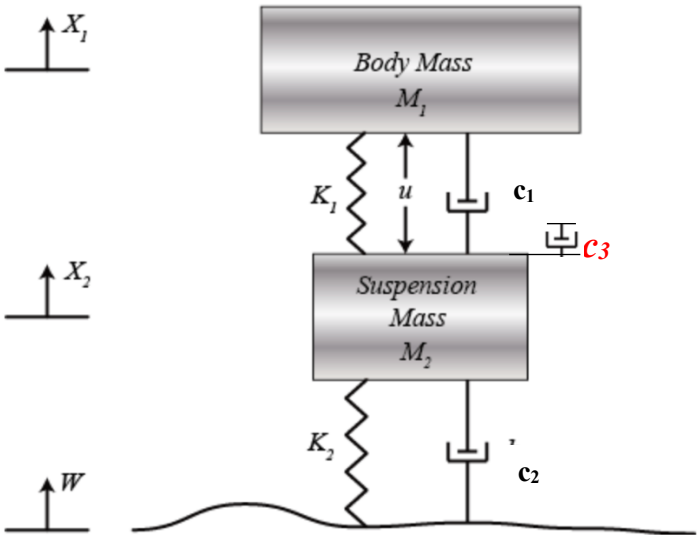

Figure 9: Half bike model with bottom-out damper

Using Newton's law, the following equations of motion are obtained for the suspension system without bottom-out damper:

$$M_1\ddot{X}_1 = -c_1(\dot{X}_1 - \dot{X}_2) - K_1(X_1 - X_2) \quad (1)$$

$$M_2\ddot{X}_2 = c_1(\dot{X}_1 - \dot{X}_2) + K_1(X_1 - X_2) + c_2(\dot{W} - \dot{X}_2) + K_2(W - X_2) \quad (2)$$

where M_1 = body mass or mass of bike and rider (kg)

M_2 = suspension mass or mass of wheel and fork (kg)

K_1 = suspension spring stiffness (N/m)

K_2 = tyre spring stiffness (N/m)

c_1 = suspension damping coefficient (Ns/m)

c_2 = tyre damping coefficient (Ns/m).

The natural frequency describes the rate at which the undamped system would freely oscillate for a given input. Typical natural frequencies for vehicle suspension range from 1-5 Hz for the sprung mass and 10-30 Hz for the unsprung mass (Kasprzak 2014). The natural frequencies for each mass can be found from analysis of the system equations of motion:

$$f_n\,(M_1) = \frac{1}{2\pi}\sqrt{\frac{(K_1K_2/(K_1+K_2)}{M_1}} \quad (Hz) \tag{3}$$

$$f_n\,(M_2) = \frac{1}{2\pi}\sqrt{\frac{K_1+K_2}{M_2}} \quad (Hz) \tag{4}$$

The damping ratio is defined as the ratio between the damping constant and critical damping. The damping ratio describes how the oscillations of a system decay to a steady state. Mathematically the damping ratio for each mass is given by:

$$\zeta(M_1) = \frac{c_1c_2(c_1+c_2)}{2\sqrt{(K_1K_2/(K_1+K_2)M_1}} \tag{5}$$

$$\zeta(M_2) = \frac{c_1+c_2}{2\sqrt{(K_1+K_2)M_2}} \tag{6}$$

When $\zeta > 1$ the system is overdamped, and no oscillations occur. When $\zeta = 1$ the system is critically damped and provides the fastest return to a steady state. For the case when $\zeta < 1$, the system is underdamped, and the response oscillates as occurs for suspension systems. A single oscillation occurs at a damping ratio of approximately 0.7, which is considered a good

reference point for suspension design. Typically, damping ratios for vehicle suspension range from 0.2 for passenger cars to 0.7 for racing applications (Kasprzak 2014). The damped natural frequency may also be determined from the above properties as:

$$f_d = f_n\sqrt{1-\zeta^2} \quad (Hz) \tag{7}$$

When initial conditions are zero for all displacements, the spring-mass-damper model represents a scenario where the wheel moves upward when it encounters a bump. The equations of motion can be represented as a transfer function by taking the Laplace transform and algebra manipulation. The transfer function relating travel $X_1(s)$-$X_2(s)$ to a displacement disturbance W(s) can be expressed as:

$$G(s) = \frac{X_1(s)-X_2(s)}{W(s)} = \frac{-M_1c_1s^3-M_1K_2s^2}{\Delta} \tag{8}$$

where

$$\Delta = M_1M_2s^4 + (c_1(M_1+M_2)+c_2M_1)s^3 + (c_1c_2+M_1(K_1+K_2)+M_2K_1)s^2 + (c_1K_2+c_2K_1)s + K_1K_2$$

This transfer function describes the suspension displacement as a function of the input disturbance in the Laplace domain (derivation is included in appendix A). It is a useful form to numerically model the suspension fork without the bottom-out damper and analyse its transient response characteristics. The damping properties outlined above are calculated for typical mountain bike parameters from the transfer function using Matlab in the simulation chapter. With the bottom-out damper, the value of c_1 is increased when the travel approaches a limit at zero. Further analysis of the transfer function is possible using a control systems approach such as the root locus method. This would provide insight into how the poles of the system move when the parameters are varied and as a result the characteristics of the response change. A brief root locus analysis has been included in appendix B. It remains beyond the scope of this design project but is useful for future designs involving active suspension control and presents an interesting avenue for future research. For the design in question here, many parameters are constrained to a small range because of the requirement to integrate the design with existing suspension products. Sufficient analysis to inform design can be carried out from simulation results in the time domain, included in the next chapter.

3.2 Dynamics of the Damper

Dampers provide a resistive force proportional to velocity by restricting the flow of oil when the suspension compresses or extends. The viscosity of oil causes a pressure differential, which subsequently produces a force acting on the piston. The pressure drop dissipates kinetic energy from a disturbance or that stored in a spring as heat. As discussed, dampers can be designed to a specific damping constant, providing control of the damping force in dynamic conditions.

3.2.1 Damper motions

The damper moved in two directions in operation: compression, when travel is decreasing, and rebound (also called extension), when travel is increasing. When the damper compresses, the pressure of oil in the damper body in front of the piston increases. Oil in the damper body passes through the valve, generating a force with direction opposing the damper motion (figure 4). For rebound of the piston, a similar process occurs in reverse. Pressurised oil behind the piston passes through the valve as the suspension and spring extends. Damper motions are illustrated in figure 10.

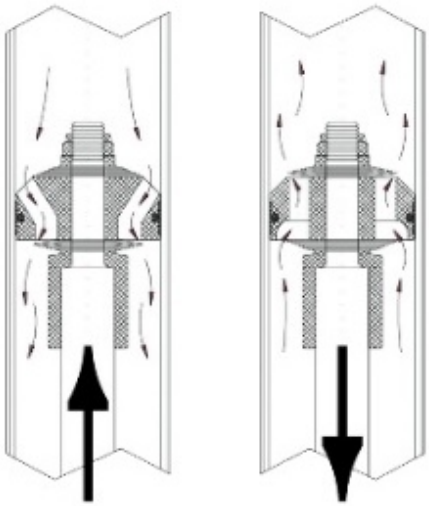

Figure 10: Compression (left) and rebound (right) damper motions (Kasprzak, 2014)

3.2.2 Cavitation

Cavitation is a phenomenon that occurs in dampers when the pressure of oil drops below its vapour pressure resulting in the formation of gas bubbles within the fluid. Cavitation degrades damper performance and accelerates the wear of internal components due to rapid phase changes of the fluid when pressure cycles. Gas at high pressure in a separate reservoir and the

internal floating piston (see section 2.5.5) is used to prevent cavitation from occurring by pressurising the fluid throughout operation of the damper.

3.2.3 Compressibility

Though liquids are typically considered incompressible in fluid analysis, they do demonstrate a small degree of compressibility in practice. This can change fluid properties such as density and viscosity and accordingly effect damping performance. However, density and viscosity variation in saturated liquid oil has been measured as less than 0.1 % and 3% per MPa respectively (Dixon 2007). Hence, for the purpose of this damper design it is appropriate to neglect compressibility effects.

3.2.4 Temperature

Energy associated with the damping force is dissipated as heat. Some of this heat is transferred into the oil used in the damper which can alter its fluid properties. The viscosity of oils is inherently dependent on temperature and as a result damping forces are also temperature dependent. Mountain bike suspension can reach high temperatures because of the large velocities experienced by the damper. Along with size and weight constraints, temperature provides a practical limit on the damping force that can be generated in a bicycle damper.

3.3 Fluid Dynamics

Fluid dynamics should be considered to guide design of the bottom-out damper. In particular, theory encompassing flow regimes, conservation of mass and momentum, entry and exit losses and Bernoulli obstruction theory are outlined in relation to damper design.

3.3.1 Flow regimes

Reynolds number is a dimensionless flow parameter used to describe the nature of fluid flow. Three flow regimes are identified to describe and analyse the behaviour of fluids: laminar, transitional and turbulent. These are defined using Reynolds Number, a dimensionless flow parameter that describes the ratio of inertial resistance to viscous resistance for a flowing fluid.

Mathematically:

$$Re = \frac{uL}{\nu} \tag{9}$$

where u = relative fluid velocity (m/s)

L = characteristic length/diameter (m)

ν = kinematic viscosity of fluid (m^2/s).

Accepted values of Reynolds number relating to internal flow for the three flow regimes are:

- Laminar: $Re_D < 2300$, steady, smooth flow dominated by viscous forces;
- Transitional: $2300 < Re_D < 2600$, flow behaviour intermediate to laminar and turbulent; and,
- Turbulent: $Re_D > 2600$, flow is unsteady, churning with vortices and dominated by inertial forces (Schobeiri 2014).

The Reynold's number will commonly determine the friction factor, and consequently pressure loss, in pipe flow which is of relevance to the damper. However, the effect of friction factor is only significant for flows of a sufficient length and flows in the damper seldom exceed a few diameters. The friction factor is assumed to have insignificant impact on pressure loss compared to minor losses. The Reynolds Number is highlighted here only as relevant knowledge to inform the design. Given the kinematic viscosity of a typical suspension fluid (15 mm^2/s) and a maximum damper passage diameter of 5 mm, flow will be laminar for fluid velocities less than 6.9 m/s. Velocities of this magnitude are very unlikely for the mountain bike fork, so it is expected that the damper will usually operate with laminar flow.

3.3.2 Bernoulli Equation and Conservation of Mass

The conservation of mass states that for a given control volume the sum of mass entering a system must equal the sum of mass leaving. By extension, Bernoulli equation expresses conservation of energy in a fluid flow. It is valid for a given stream line under the assumption of constant density.

For small height changes and neglecting major losses due to friction, the Bernoulli equation can be expressed as:

$$P_1 + \frac{1}{2}\rho {u_1}^2 = P_2 + \frac{1}{2}\rho {u_2}^2 + \Delta P_{st} \quad (10)$$

where P = pressure (Pa)

ρ = desnsity (kg/m^2)

ΔP_{st} = stagnation pressure change to account for minor losses (Pa).

This forms the basis for estimation of the damping coefficient from damper geometry provided below.

3.3.3 Minor losses

Minor losses due to changes in flow area or direction affect fluid flow in a damper. Specifically, entry losses are caused by small vortices forming inside the contraction of an oil passage. This is inherent in damper design as suspension oil is forced through a small port to generate a damping force. Entry losses occur when the flow area is reduced to less than that of the diameter of the passage. Vortex generation can be reduced by providing a more gradual change in section such as rounding the entranceway. Exit losses are a result of sudden expansion in section and will be present in damper design where oil leaves a port and enters a reservoir. Similarly, a more gradual section change can reduce the formation of vortices that can result in pressure loss and unpredictable damper performance. To limit minor losses, consideration of flow behaviour will be taken in design of the damper.

3.3.4 Calculation of damping coefficient

Analytical equations have been derived from fluid theory to calculate the damping coefficient, c, for a particular damper geometry (Schobeiri, 2014). For the piston type damper shown in figure 11 and assuming laminar flow in the capillary of diameter d and length L, the damping coefficient can be approximated as follows:

$$c = 128\pi\mu L\left(\frac{R_0}{d}\right)^4 \quad \text{[Ns/m]} \qquad (11)$$

where μ = dynamic viscosity of the fluid (Pa·s).

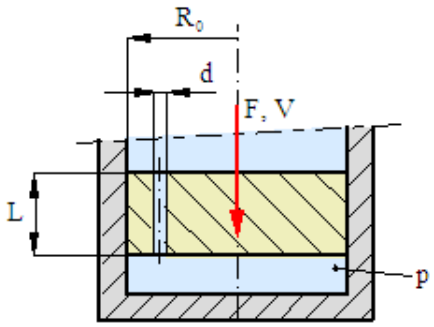

Figure 11: Piston viscous damper geometry

Despite the assumptions made, this will be used as the best approximation to estimate the damping coefficient for the prototype design and predict the system response of the suspension fork in later chapters.

4 Simulation for Design

Matlab Simulink was used to develop a bicycle front suspension model from theory and demonstrate the response of the system to various inputs. This section describes development of the model and evaluates potential solutions to the bottom-out problem from simulation results. The simulation confirms advantages of a bottom-out damper and offers guidance for the physical design.

4.1 Methodology

The model was based on a two degree of freedom mass-spring-damper system and theory identified in the previous chapter. The assumptions supporting the model, limitations and Simulink modelling process are outlined below.

4.1.1 Assumptions

There are two underlying assumptions in the spring-damper model:

- springs provide a force proportional to displacement; and,
- dampers provide a force proportional to velocity.

Table 1 provides values assigned to system parameters and their physical meaning. These were based on actual values and estimates from existing studies.

Table 1: Suspension parameters for simulation

Name	Description	Variable	Value
Body Mass	Bicycle and rider mass completely distributed on front wheel in extreme case	M_1	91 kg
Suspension Mass	Front fork, wheel and tyre mass	M_2	4.5 kg
Suspension Spring Constant (stiffness)	Corresponds to Rockshox Extra Firm fork spring	K_1	8.7 kN/m
Tyre Spring Constant (stiffness)	Tyre stiffness from literature (Jianmin, Gall & Zuomin, 2001)	K_2	150 kN/m
Compression Damping Constant	Estimated, including friction component	b_1	900 Ns/m
Tyre Damping Constant	Tyre damping from literature (Jianmin, Gall & Zuomin, 2001)	b_2	70 Ns/m
Rebound Damping Bias	Gain applied to compression damping in rebound	reb	1.2
Bottom-Out Damping Gain	Gain applied to compression damping in bottom-out region	bot	1-5
Disturbance bump height	Amplitude of ramp function used to model bottoming impact	h	0.3 m

4.1.2 Limitations

There are inherent complexities in many suspension designs that are difficult to model and have been excluded from the simulation. Also, there are limitations modelling real life operating conditions. The following are further discussed below:

- non-linear air springs;
- non-linear damping;
- constraints on input; and,
- computational limitations.

Many suspension products use air springs, which provide a force that is not linearly dependent on displacement. Additionally, air springs rates are temperature dependent. Since pressure is proportional to temperature of a gas (by the ideal gas law), more force is required to compress air at higher temperatures. Despite air springs offering greater adjustability and weight advantages, linear coil springs are generally preferred for downhill mountain biking. They provide greater consistency in varying conditions and therefore used in the simulation. Tyres are also modelled as linear elastic springs for simplicity, whereas in reality they also demonstrate non-linear properties of air discussed above. This is likely to have a negligible impact on results due to the relatively high stiffness associated with the tyres.

Some suspension designs seek greater control over damping by using complex valving, independent high and low speed damping circuits and other means that result in a damping force not directly proportional to velocity as assumed by the model. For example, threshold valves are used to permit greater fluid flow (and lower damping force) only when a certain fluid pressure is exceeded. For simplicity, the model only accounts for a higher damping constefficient in extension (rebound) than compression. This rebound bias is present in vehicle suspension to improve control by reducing overshoot when the spring extends (Kasprzak, 2014). Additionally, friction forces acting between moving parts can lead to non-linear damping properties. Manufacturers seek to minimise friction forces using special coatings and seals with low friction coefficients. Therefore, the model assumes that all friction forces can be included in the damping force caluclation (as proportional to velocity).

Finally, the input to the system may only be approximated in the simulation and does not exactly replicate a disturbance experienced in real life. A steep ramp function is used to model the bicycle landing a vertical drop, an event when bottom-out of the suspension would typically occur. However, in real life scenarios, factors such as input from the rider and initial conditions for the suspension will affect the input and subsequent response of the system. The influence of these factors must be studied experimentally as carried out for validation of the prototype. Lastly, there are always computational limitations when discrete approximations are used to model a continuous time system. The resulting computational error is considered negligible for the context of this simulation.

4.1.3 Damped System Characteristics

Characteristics of a standard mountain bike suspension system with constant damping were calculated according to theory, using the assumed suspension parameters. Table 2 describes the predicted natural frequency and damping characteristics for typical mountain bike suspension. Matlab code is included in appendix C.

Table 2: Damped system characteristics

Mass	Natural Frequency (Hz)	Damping Ratio (ζ)	Damped Natural Frequency (Hz)
Body mass (bike)	1.60	0.48	1.41
Suspension mass (wheel and fork lower)	29.9	0.59	23.4

The damping ratio indicates an underdamped response, with the suspension oscillating more than once for a given input. Since the sprung mass has a much lower natural frequency, this mode will dominate the response for the lower frequency inputs expected for suspension.

4.1.4 Simulink Model

A Simulink model was built with the input and outputs shown in figure 12 and block diagram configuration in figure 13.

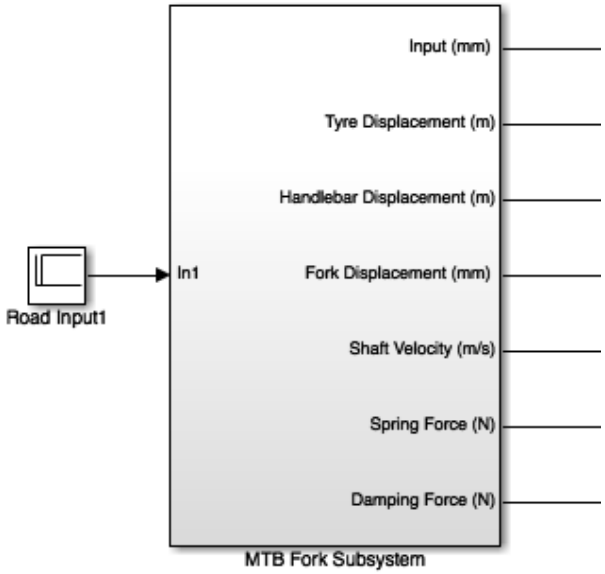

Figure 12: Simulink suspension fork model

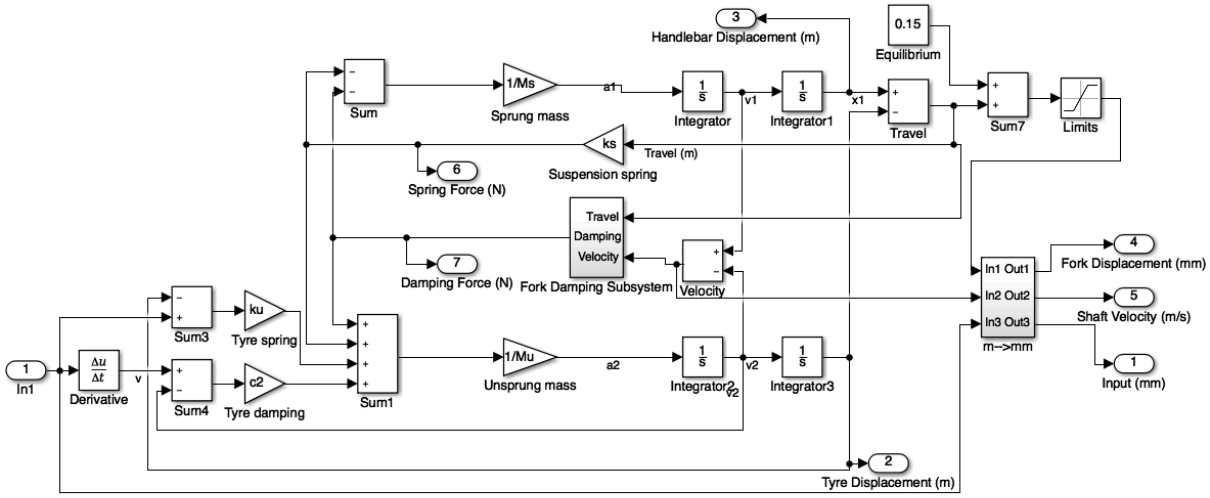

Figure 13: Simulink block diagram

The fork damping subsystem adjusts the damping constant depending on the sign of velocity to incorporate a rebound damping bias. The subsystem was also modelled using feedback conditional on travel so as to increase the coefficient c_1 and hence the damping force when travel approaches full compression. Further subsystem design is included in appendix D.

The response of the system to a steep ramp input were observed for the following cases:

- **default** values with bottom-out occurring;
- **increased spring stiffness** to prevent bottom-out;
- **increased damping** to prevent bottom-out; and,
- **bottom-out damper** to prevent bottom-out (increased damping in final 50 mm of compression).

By changing these variables individually, different methods to address bottom-out were compared. A small variation observed in the response to the single disturbance in the model may be considered to accumulate in real life over the course of an entire mountain bike trail, producing an aggregate effect that significantly effects performance.

4.1.5 Criteria for evaluation

A set of criteria were defined to evaluate suspension performance from the results of the simulation (and subsequently during prototype validation). These can be summarised under the categories of comfort and control. While often competing objectives in suspension design, for this project an improvement in suspension performance is identified by improving one of these aspects without making the other worse. Table 3 describes how comfort and control can be assessed from the system response and physical equivalence in a mountain bike context.

Table 3: Criteria for evaluating suspension performance

Comfort	Control
Prevent bottom-out to limit force transmitted to rider.	**Prevent bottom-out** to limit force transmitted to components.
Reduce response time (time to maximum compression) to decrease velocities experienced by the rider.	**Prevent full extension** to maintain tyre-ground contact and prevent loss of traction.
Increase settling time to reduce accelerations experienced by rider.	**Reduce settling time** to achieve more constant normal force between tyre and ground (improve traction).

Eliminating bottom-out is advantageous to both comfort and control and the first priority of the design project. However, this should be achieved by minimising trade-offs with other performance objectives.

4.2 Simulation Results

Results from the simulation are presented below and discussed with reference to the criteria. Additional graphs of simulation results including outputs other than displacement are included in appendix E. The ground disturbance used to simulate a bottom-out event is shown in figure 14. The steep ramp input models a scenario when a mountain bike lands a jump or drop-off and full compression would typically occur.

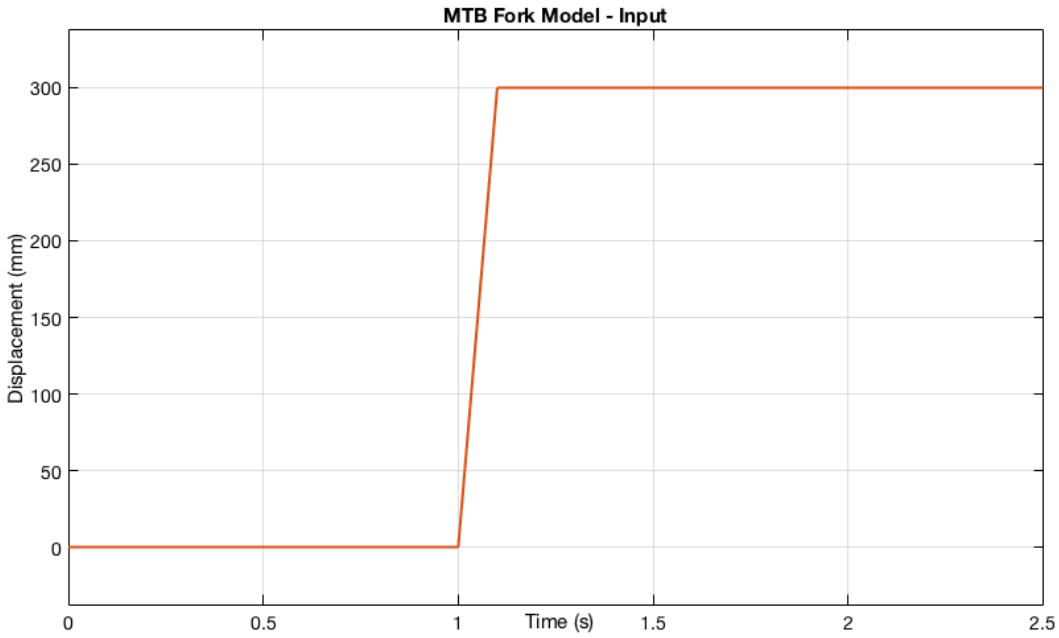

Figure 14: Disturbance input

4.2.1 Existing solutions

Figure 15 shows the displacement response for the model of a standard fork experiencing full compression (default) compared to the response when damping or spring stiffness are increased by a factor of two to prevent this bottom-out. The upper limit of travel (full extension) is constrained to 200 mm and static equilibrium is at 150 mm displacement.

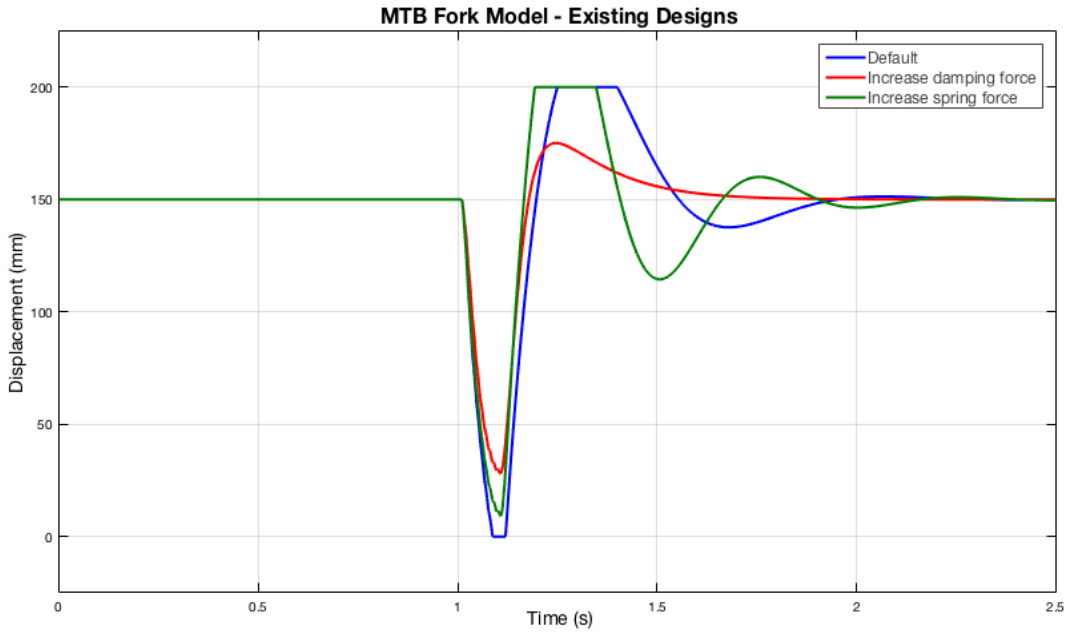

Figure 15: Existing designs - displacement response

The default response in blue shows travel decreasing to zero (full compression), then extending to full extension for approximately 0.2 seconds before returning to static equilibrium approximately one second after the disturbance with a single damped oscillation. The flat section at full extension can be physically interpreted as a period when there is no force acting between the front tyre and ground. The tyre has 'bounced' and is no longer in contact with the ground which would result in a lack of traction, reducing control.

The response in red, with increased damping force shows a slightly slower compression of the suspension in response to the disturbance. This would result in the rider experiencing comparatively more force due to the impact versus the standard response, which is detrimental to comfort. Bottom-out is successfully prevented with a larger damping force, as is full extension and the fork quickly returns to static equilibrium 0.7 seconds after the bump. This faster settling time has control advantages since a more constant normal force between the tyre and ground is achieved but also has comfort trade-offs. The rider experiences higher accelerations to achieve the faster return to equilibrium. Lastly, there are design issues with significantly increasing the damping constant throughout the forks travel. Since more energy is dissipated in this condition, the fork would operate with higher pressures and temperatures.

Increasing the spring force to eliminate bottom-out, shown in green, demonstrates a similar displacement response to the standard fork but with an initially lower amplitude of compression. It results in a relatively less damped response (the natural frequency is higher) and longer settling time. Full extension is achieved more quickly after the disturbance, resulting in a lack of traction. The longer settling time also negatively impacts control as the normal force permitting traction varies quickly as long as the oscillations persist.

4.2.2 Bottom-Out Damper

Figure 16 shows the default displacement compared to the bottom-out damper case. The displacement initially follows that of a standard suspension fork until increased damping below 50 mm displacement prevents bottom-out. Since less elastic energy is stored in the spring, the fork does not fully extend and therefore tyre-ground contact is maintained which enhances control. The fork returns to static equilibrium at a similar time as the default case. The bottom-out damper is also compared to existing solutions in figure 17.

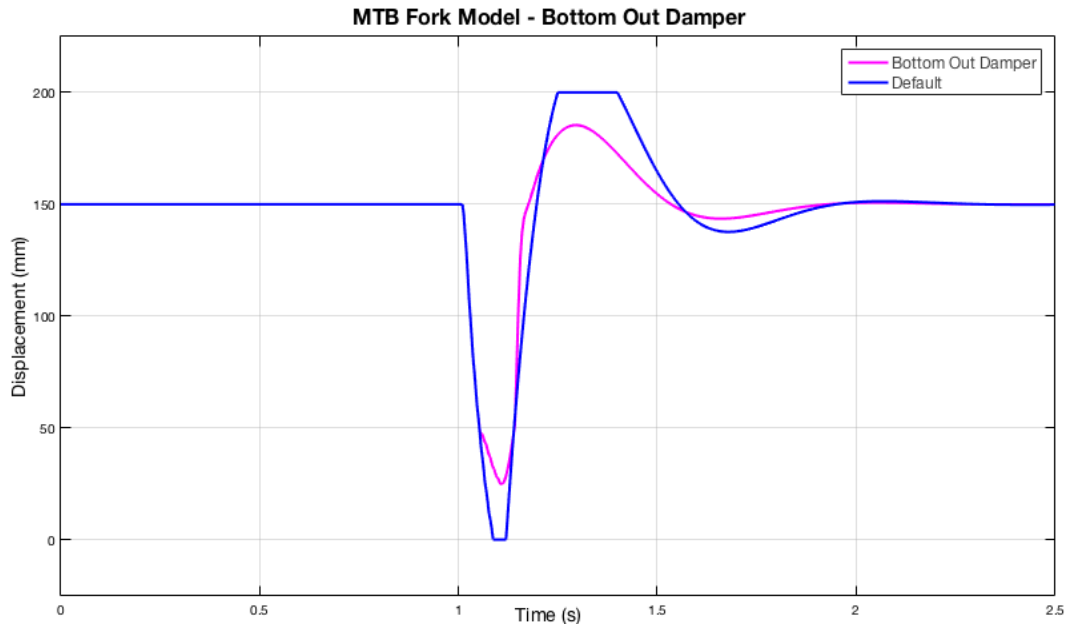

Figure 16: Bottom-out damper - displacement response

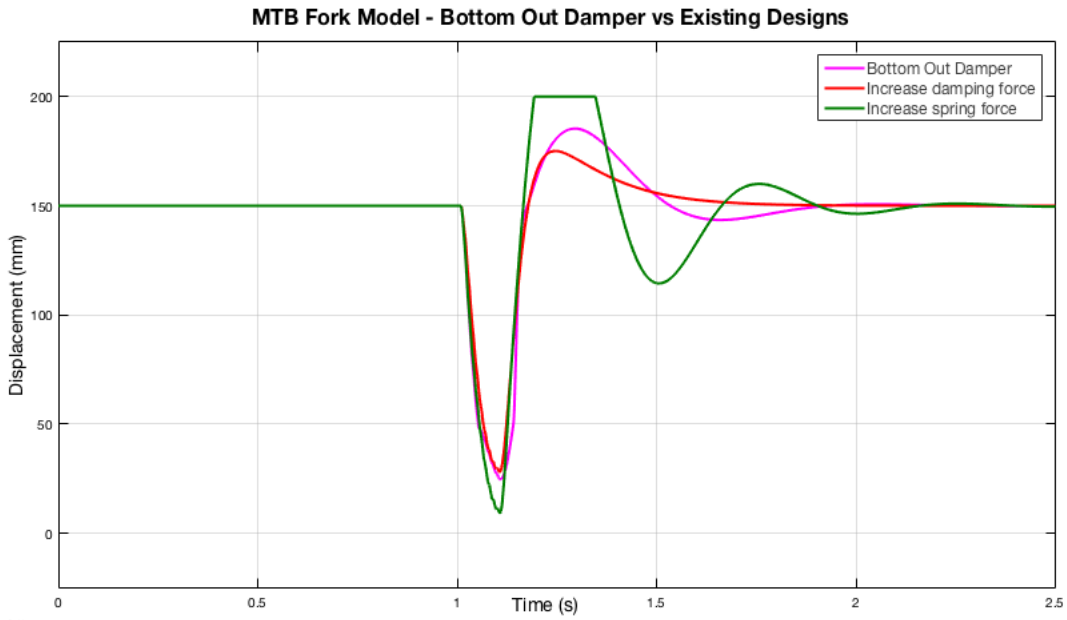

Figure 17: Bottom-out damper vs existing designs

4.2.3 Repeated Impacts

A continuous stair disturbance as shown in figure 18 was used to simulate the response of the bottom-out damper and standard suspension fork to repeated impacts. The magnitude of the step decreases to model two initial bottoming impacts followed by smaller 'bumps'.

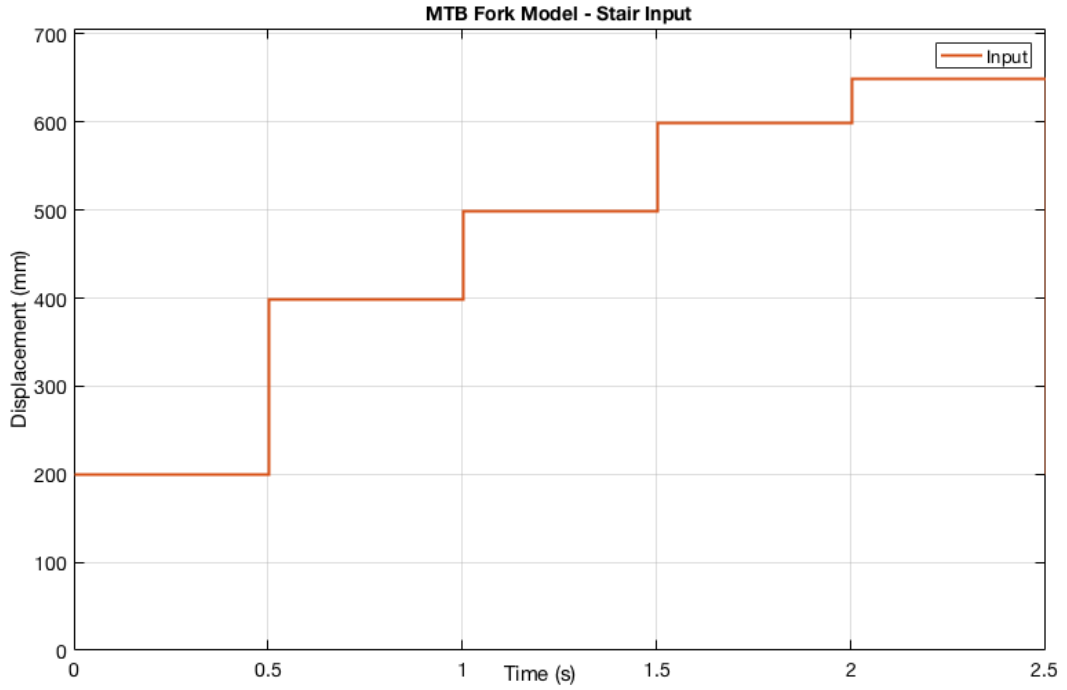

Figure 18: Repeated disturbance input

The resulting displacements are shown in figure 19. These results demonstrate the damper prevents bottom-out and reduces rebound overshoot of the fork only when bottom-out would otherwise occur. For the smaller impacts following, the two responses are almost equivalent. This implies there is no performance trade-off from using the bottom-out damper under smaller impacts for which the standard fork is optimised.

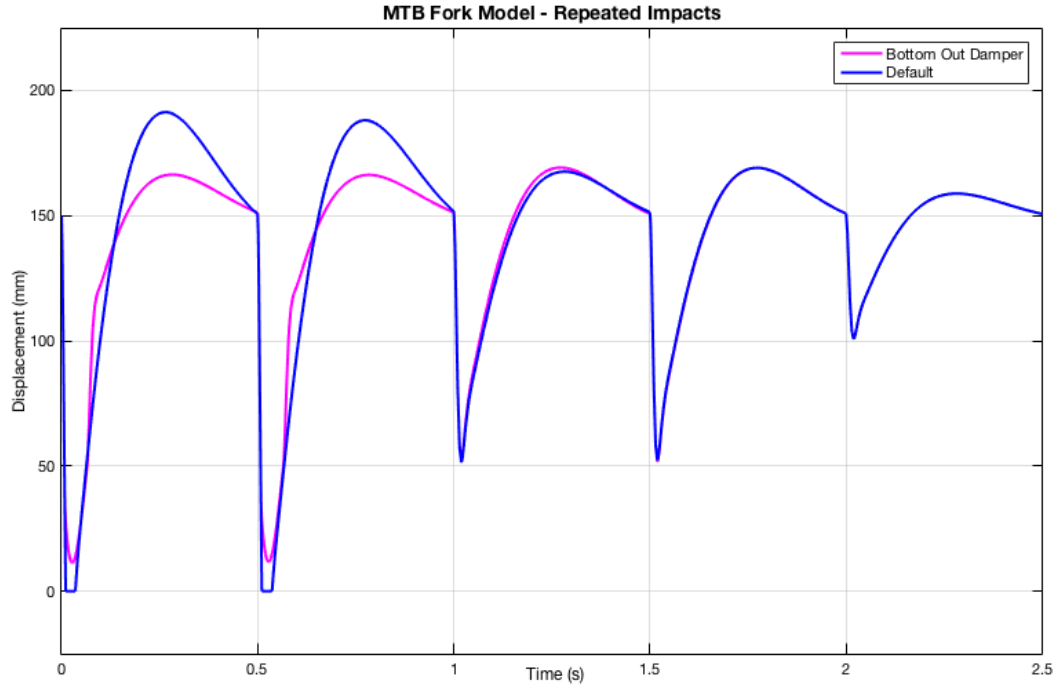

Figure 19: Bottom-out damper - repeated impacts

4.2.4 Summary of simulation

Table 4 summarises the performance of suspension under different solutions to address bottom-out according to the criteria.

Table 4: Simulation Results

Design	Prevent bottom-out	Response Time	Eliminate full extension	Settling Time	Overall Performance
Default Fork	✗	0.15 s	✗	1 s	Baseline
Increased Spring Stiffness	✓	0%	✗	+30%	Comfort bias (Control trade off)
Increased Damping	✓	+8%	✓	-25%	Control bias (comfort trade off)
Bottom-Out Damper	✓	+0%	✓	+0%	Comfort and Control (no trade off)

The bottom-out damper design avoids trade-offs inherent in existing methods to prevent full compression (figure 17). It is possible that a combination of increased spring stiffness and increased damping may be used to achieve similar results as the bottom-out damper. However, this approach still increases the response time (dependent on damping) and reduces the suspension's ability to react to small impacts when bottom-out is not a concern, which is not specifically addressed in the above criteria. The damper is advantageous in this sense, as it only changes the dynamics of the system when the suspension is almost fully compressed and there is a risk of bottom-out occurring. This is further illustrated in the results for repeated impacts in figure 19 and additional results in appendix E.

4.3 Considerations for Design

The bottom-out damper should substantially increase the damping constant near full compression. A gain of three to five times the existing compression damping force was sufficient in the model. The device should only influence dynamics when the fork is near full compression or it risks significant performance trade-offs faced by existing solutions. The damper may also interfere with non-linear suspension characteristics identified in the limitations of this simulation. This could explain discrepancy between theoretical and experimental results. Nonetheless, the simulation affirmed the proposed damper as a more optimal method to address bottom-out than the current available means. The simulation is repeated using parameters from the final prototype design and test suspension rig in the validation chapter. Furthermore, predicted results are compared to experimental test results, which may provide insight for development of an improved bicycle suspension modelling in the future.

5 Prototype Damper Design

This section describes the entire design process and manufacture of a mountain bike bottom-out damper. Functional requirements are identified and met by design and selection of appropriate components, materials and manufacturing techniques.

5.1 Design Considerations

The primary function of the bottom-out damper is to provide additional damping force at the end of the suspension stroke that is adjustable over a wide range to suit various conditions. When active, the damper reduces displacement for a given impact by converting kinetic energy into heat as oil is forced through small orifices. This will prevent harsh bottom-out forces from being transmitted into the rider or frame and improve recovery of the suspension to equilibrium for subsequent impacts. To be externally adjustable, the design must consider how the flow of oil is metered when the fork is compressed. The major constraint is that the device must seamlessly integrate with a Rockshox suspension fork with 35 mm stanchions without inhibiting existing mechanisms. Functional requirements and considerations for the design are summarised below.

5.1.1 Functional Requirements

Qualitatively the bottom-out system should be easy to install and remove, have a wide, usable range of adjustment and be lightweight. It should also comprise of few parts for simplicity and fail safely without risk of injury or damage to other equipment. The damper should also appear congruent with the fork and be unsusceptible to potential impacts such as rock strikes. The functional requirements are quantified where possible in table 5.

Table 5: Functional Requirements

Function	Engineering Requirement	Metric	Source
Budget	Cost	< $300	Customer
Performance	Maximum shaft velocity	2m/s	Customer
	Damping at closed position	Hydraulic lock prevents bottom-out	Industry
	Damping at open position	< 100 Ns/m	Industry
	Range of adjustment	> 10 settings	Customer
Design	Mass	< 250 g	Customer
	Part count (simplicity)	< 7 parts	Industry
	Volume	80 cm^3	Industry
	Time required to adjust	10 seconds	Customer
	Time required to install/uninstall	20 minutes	Customer
	Bolt sizing	M8 (ISO)	Industry
	Rebound adjustment tooling (Hex)	2.5 mm Hex	Industry
	Damping adjustment tooling	By hand	Customer
	Minimum Operating temperature	-20 °C	Customer
	Maximum Operating temperature	80 °C	Customer
	Frontal impact resistance	100 kN	Customer
	Diameter of oil port	4 mm	Industry
	Maintenance interval	50+ hours	Customer

5.1.2 Durability

The damper must be durable to ensure a long operating life and provide consistent performance. It is beneficial to be able to repeatedly adjust the device, install it and disassemble components, all of which can cause wear. Major components should be designed to either prevent wear or continue to be functional when wear occurs. There will be a trade-off between durability and weight. Durability should be achieved, and fatigue life extended as far as possible while meeting the target mass of less than 250 grams. Higher tolerances on machined parts and stronger materials will improve the durability of the damper but also incur greater financial cost. A cost constraint for the damper is set at $300 for this reason.

5.1.3 Cost

The overall cost of the prototype damper is likely to be much higher than a future production for multiple units due to economies of scale. Consideration of cost in design can reduce the cost of manufacturing one-off components. Simpler geometries and standard tooling can be adopted for the prototype with additional non-critical detail added if the damper progresses to production.

5.1.4 Manufacturability

A design is not feasible if it cannot be manufactured. What is manufacturable will depend on cost, production time constraints, materials and the complexity of design. Where possible, the damper should follow standard dimensioning and tolerances. By nature, dampers require tight tolerances to ensure predictable and accurate operation. CNC machining is suitable for manufacturing aluminium components for the bottom-out damper to a high accuracy.

5.1.5 Heat dissipation

The damper converts kinetic energy into heat by forcing oil through narrow passages. The heat generated from frictional forces when flow is restricted is then transferred into the oil and damping components. Hence, all materials should be resistant to temperatures of up to 80 ^{o}C (no property changes) and not susceptible to creep. A larger fluid reservoir and increased external surface area will increase the rate of heat transfer from the suspension oil to the environment. Using materials with a higher thermal conductivity, such as aluminium, and maximising airflow around the damper will also aid heat transfer by conduction and convection respectively. Fluid properties are dependent on temperature and affected by thermal cycling. Improving heat dissipation maintains the oil at a more constant temperature therefore resulting in more consistent damping performance. It will also extend service intervals for replacement of the suspension oil.

5.1.6 Sealing

The damper generates large internal pressures as part of normal operation. These pressures must be contained by structurally sound oil passages, adequate sealing and sufficiently strong fasteners. Typically, rubber o-rings are used to provide fluid seals when compressed between components. Tight tolerances to improve the alignment of oil passages between the fork and bottom-out damper will also benefit sealing.

5.1.7 Interface

The damper should not interfere with existing suspension mechanisms, yet it must be physically linked to compression of the fork through a shaft. Ideally the design would ensure some redundancy; if the bottom-out damper fails, the suspension fork would continue to function. In particular, rebound adjustment is located at the bottom of the fork leg and should remain externally accessible with the proposed damper design.

5.1.8 Installation

Consideration must be given to the ease of installing the damper on an existing suspension fork. In order for it to appeal to consumers, the damper should not be technically challenging to install. This means it takes a short amount of time to install, uses standard tooling, is easily accessed and can be achieved with simple instructions. Similarly, the damper should be easily removed from a bike.

5.1.9 Maintenance

The design should ensure ease of disassembly to allow servicing at home for the average rider. Internal adjustment of the damper may be carried out at the time of servicing to provide greater control over adjustment than available externally. Additionally, the damper should be designed for a service interval of at least 50 hours. This is the manufacture recommended interval for servicing the lowers of a Rockshox suspension fork.

5.2 Design Overview

In brief, the prototype damper is required to increase the damping force as the fork nears the limit of its travel. This can be achieved by restricting the flow of oil by forcing it through a small sectional area. Existing damper components that provide such flow restriction are readily available in the industry and will be employed in the design. The main design challenge remaining is incorporating a damper into an existing suspension fork. Figure 20 shows an exploded view of the right leg of the Rockshox Boxxer Fork.

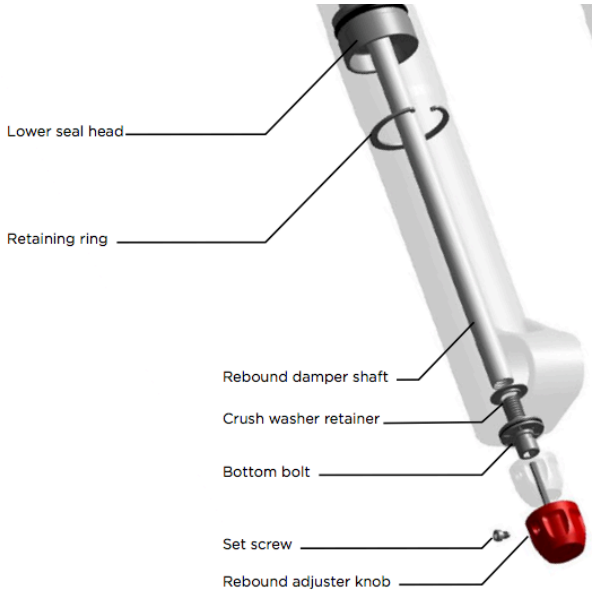

Figure 20: Rockshox Boxxer right leg - exploded view (Rockshox, 2017)

The bottom-out device must be integrated into this zone without inhibiting existing parts or functions of the suspension. A damper body external to the suspension fork was the only means to achieve this without compromising durability by using excessively thin materials in an internal damper. The proposed design would permit suspension oil to flow out the bottom of the fork when suspension compresses and into reservoir housing a damper. This configuration is inspired by a similar prototype design by BOS engineering that employed an external reservoir, shown in figure 21. In this case, the external chamber was an air chamber and not a damper. For the design, an existing mountain bike rear shock damper reservoir was used as the damping mechanism (including external adjuster) shown in figure 22. Therefore, the design focuses on ensuring predictable flow of suspension fluid in and out of the damper body at the last stage of compression without affecting other dynamics. This required some parts with custom geometry that integrated with existing fork components.

Figure 21: BOS suspension fork (Pinkbike, 2017)

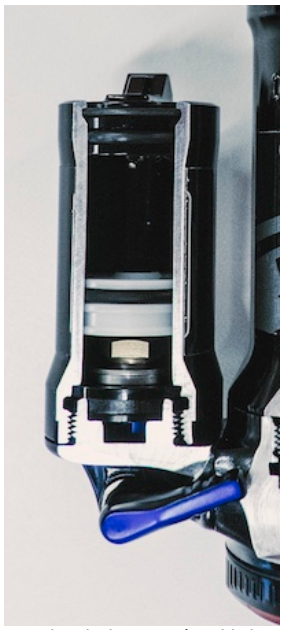

Figure 22: Rear shock damper (Pinkbike, 2017)

5.3 Components and Manufacture

Materials for the bottom-out device should be strong, durable and resistive to corrosion and permit heat transfer. The main material used is 6061 aluminium alloy due to its high strength, good workability and excellent corrosion resistance. One small part is 3D printed from ABS plastic. When required, manufacture was outsourced to a professional machining workshop with CNC capability. This allowed very high tolerances to be met and ensured a high standard of workmanship and fast turnaround. Outsourcing manufacturing tasks also reduced both project and occupational health and safety risks.

5.3.1 Component List

Table 6 lists details and functions of each component in the bottom-out design. Three components are manufactured for the damper: a bottom plate, custom bolt and spacer. These are assembled together with an existing shock reservoir which contains a shim stack and adjustment mechanism to vary the damping force as in figure 24. Pre-existing fasteners and seals were used in the assembly.

Table 6: Component list

Part	Description	Function	Notes
1	**Rockshox Super Deluxe Rear Shock Reservoir**	Includes damping mechanism – oil port metered by a shim stack with adjustable preload. Houses a gas chamber and internal floating piston to force the fluid back into the fork.	Existing suspension component procured from industry
2	**Bottom Plate**	Connects the bottom of the fork to the damper reservoir and allows suspension fluid to flow between. Attaches to reservoir by two bolts.	CNC machined from 6061 aluminium
3	**Piston**	Fits around the rebound damper shaft and forces fluid into the damper reservoir when the suspension is compressed.	Existing suspension component procured from industry
4	**Custom Bottom Bolt**	Attaches the bottom plate to the fork. Hollow bolt permitting rebound adjustment. Replaces existing bottom bolt.	Stainless steel bolt cut to size and drilled
5	**Spacer**	Fits between the lower seal head and the piston to control point when damper engages.	Printed from ABS plastic
-	**Bolts, washers and seals**	Fasteners used for assembly. Washers and seals act between surfaces to spread load and hydraulically seal the unit.	Existing parts available from market

Figure 23 shows the configuration of the bottom-out damper. There are five major components of the design (numbered). Additional parts include seals where the suspension fluid enters and exits of the bottom plate and two small bolts (M4) used to fasten the bottom plate to the shock reservoir.

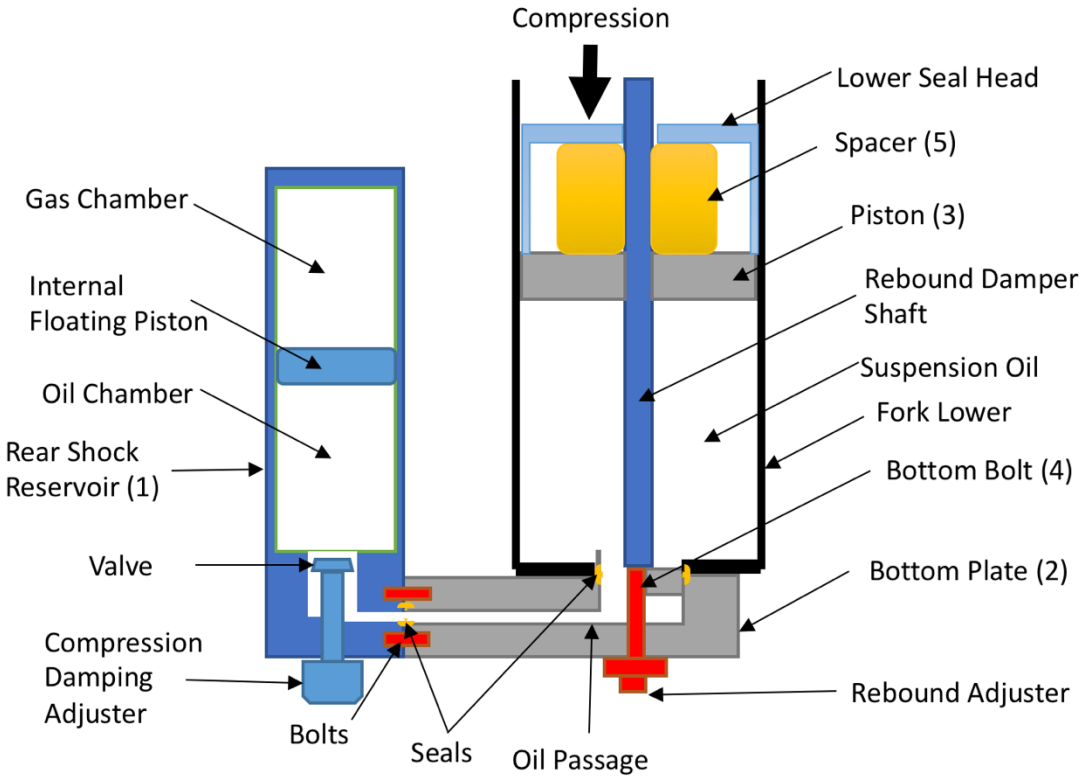

Figure 23: Bottom-out damper – section view

5.3.2 Rockshox Shock Damper Reservoir

Figure 24 and 25 show the Rockshox damper reservoir that was employed in the design. It was sourced with industry support and is commercially available as part of a Rockshox Super Deluxe rear shock. While it would be possible to manufacture these components, this project focusses on application of a damper to prevent bottom-out, not optimising the damping mechanism itself. The damper reservoir includes:

- a compression assembly with shim stack for controlling oil flow;
- an external dial (compression valve) that adjusts preload on the shim stack; and,
- an internal floating piston and air chamber to pressurise oil.

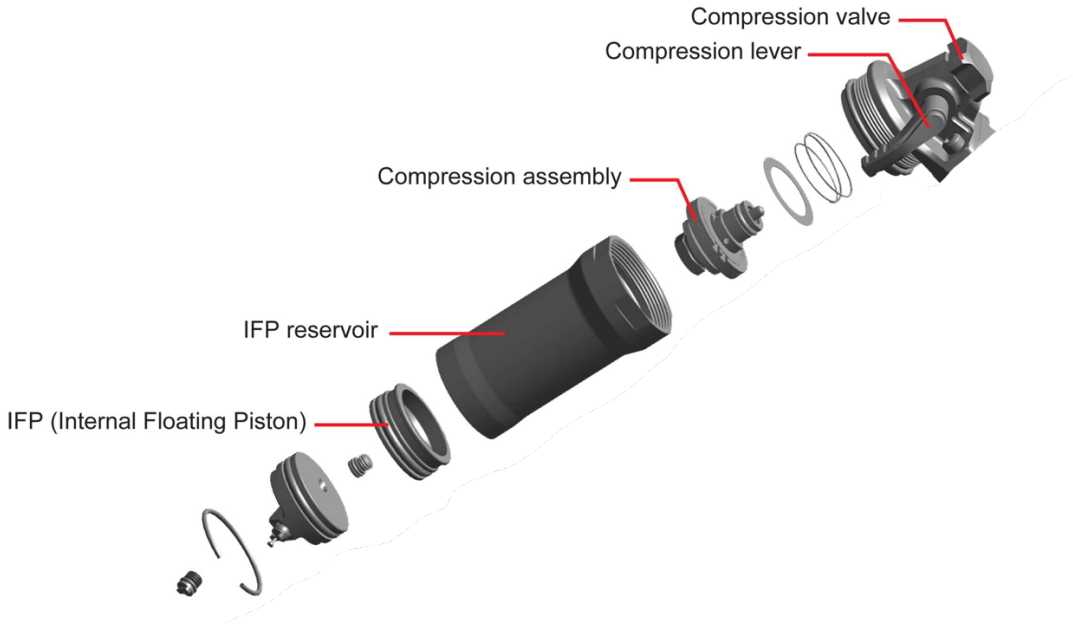

Figure 24: Rockshox Super Deluxe damper reservoir - exploded (Rockshox, 2017)

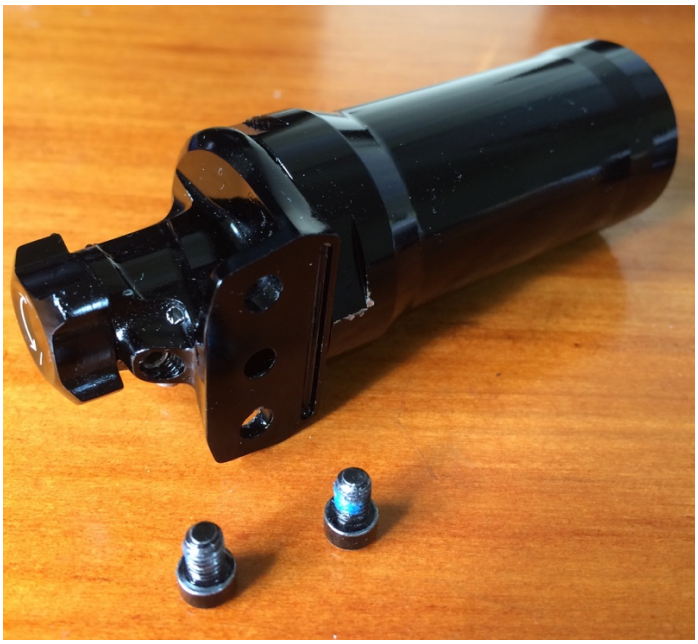

Figure 25: Rockshox Super Deluxe damper reservoir

The damping coefficient was estimated for the geometry of the valve and reservoir from theory (refer to section 3.3.4). Assumed dimensions and the result are given in table 7.

Table 7: Theoretical damping coefficient

Name	Parameter	Value
Dynamic viscosity (Castrol 10Wt Suspension Fluid)	μ	0.0132 Pa.s
Restricted flow diameter	d	0.7 mm
Restricted flow length	L	3 mm
Oil reservoir radius	R_0	13 mm
Damping Coefficient	c	1890 Ns/m

This value of damping coefficient will be used to predict the suspension response in the validation chapter.

5.3.3 Bottom Plate

The bottom plate shown in figure 26 was modelled in PTC Creo Parametric. It is dimensioned from precise measurements to accurately align with the bottom of the fork leg and the Rockshox damper body. A customised M8x1 ISO bolt to the fork and two M4x0.5 ISO bolts to the reservoir are used as fasteners. The bottom plate contains an oil passage permitting flow from the suspension fork to the external damper. Grooves are incorporated around oil ports to house rubber o-rings and ensure hydraulic sealing. The plate is designed with a rounded front facing profile to deflect impacts. The bottom plate aids heat dissipation by locating the damper body away from the suspension fork for greater airflow. Complete engineering drawings are included in appendix F.

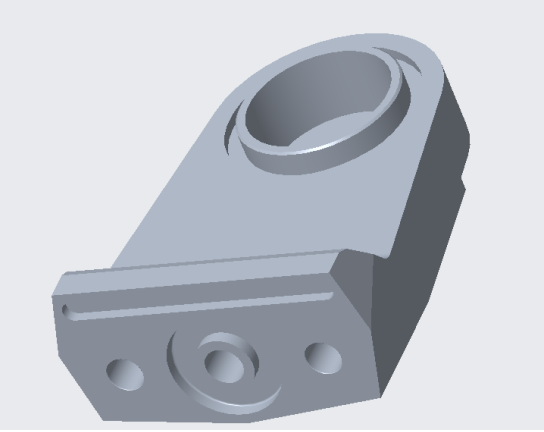

Figure 26: Bottom plate

A design with more simple geometry was CNC machined from 6061 aluminium for the prototype damper, shown in figure 27. This reduced one-off machining costs but provides equivalent function for testing and proof of the bottom-out damper concept. A rubber washer was used between the plate and fork to ensure sealing.

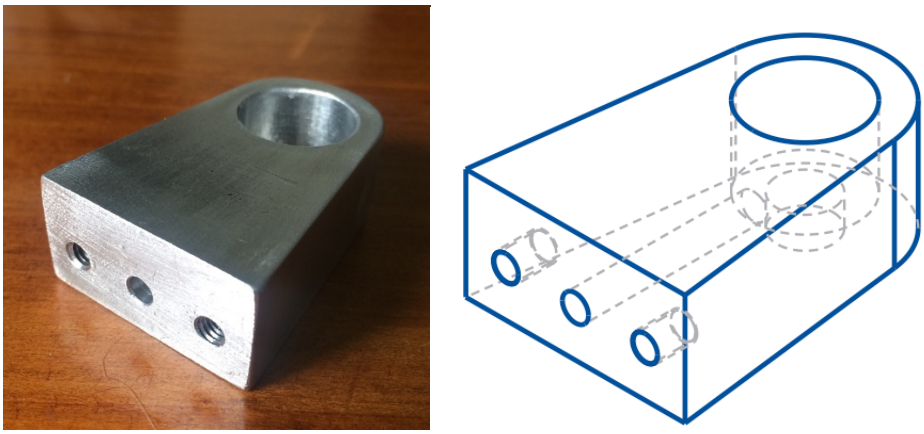

Figure 27: Prototype bottom plate

5.3.4 Piston

The piston, shown in figure 28, is a small cylindrical aluminium component used on some suspension forks. It has a 10 mm diameter internal hole that fits the rebound damper shaft and 18 mm/ external diameter that fits the bottom of the fork stanchion. It houses both an inner wiper seal and external o-rings. These seals minimise friction so that the piston can slide down the rebound shaft when the fork is compressed, maintaining a hydraulic seal so that oil is forced from the bottom of the fork leg into the damper.

Figure 28: Piston

5.3.5 Bottom Bolt

The custom bottom bolt (figure 29) mimics the existing bottom bolt used on a suspension fork but increases its length to compensate for the height of the bottom plate. It is hollow to permit access for a 2.5 mm Hex to adjust rebound damping in the fork. The bolt is shown fitted with a nylon crush washer to ensure sealing.

Figure 29: Bottom bolt

5.3.6 Spacer

Figure 30 shows the cylindrical ABS plastic spacer that can be manufactured by 3D printing. It fits within the fork leg on the rebound shaft above the piston to ensure the correct amount of oil is displaced when the fork approaches full compression. A larger spacer would cause the bottom-out damper to engage at an earlier stage in compression. Varying the height of the spacer allows the design to be compatible for several Rockshox fork models. For a Rockhox Boxxer fork, spacer dimensions are 16 mm diameter by 18 mm height, whereas the shorter travel Rockshox Lyrik fork used to test the prototype requires no spacer.

Figure 30: Spacer

5.4 Design Summary

The assembled damper is shown installed on a mountain bike in figure 31. An installation guide is included in appendix G.

Figure 31: Prototype bottom-out damper on Rockshox Lyrik fork

Specifications for the manufactured prototype damper are given in table 8. Additional design specifications are included in appendix H.

Table 8: Design specifications

Description	Specification
Part count	8 (including fasteners)
Mass*	188 g
Volume	68 cm^3
Materials	6061 Aluminium, ABS plastic
Valve type	Shim stack
Damping adjustment	Preload adjustment, 12 positions
Bolt specifications	One M8x27 mm (custom - hollow) Two M4x8 mm (fine thread)
Required oil volume (Castrol 10Wt)	60 mL
Tooling for installation^	1.5, 2, 3, 5, 6 mm Hex drivers Rockshox suspension syringe Rockshox IFP valve adapter Rockshox shock pump
Cost#	$320

* Not including oil, see also appendix H.

^ Additional tooling is required for complete disassembly of the damper.

This cost does not include the value of components provided by industry.

Operation of the bottom-out damper is described in the following steps and figure 32:

1. The fork compresses towards bottom-out, forcing the piston downwards on the rebound shaft.
2. The piston displaces oil out the bottom of fork leg and into the external reservoir.
3. Pressurised oil flows through the valve in the external damper generating a resistive damping force.
4. The internal floating piston moves upward in the reservoir, compressing air in the gas chamber, to accommodate increased oil volume in the damper.
5. The fork extends due to stored elastic energy in the spring. The internal floating piston returns oil through the damper and into the fork leg due to a pressure differential.

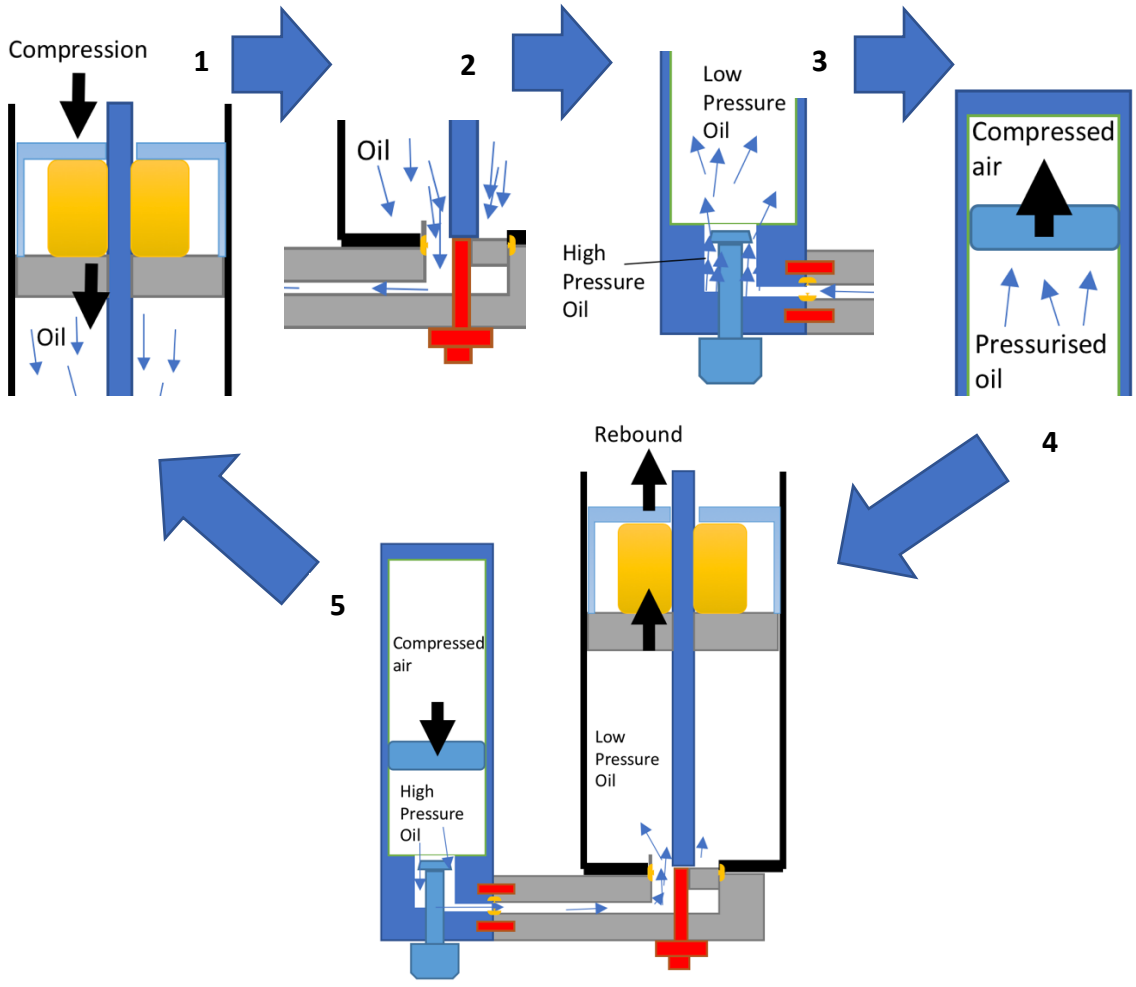

Figure 32: Operation of the Bottom-Out Damper

The bottom-out damper was designed and manufactured in a very short time frame. This rapid process followed expectations in the racing industry, companies compete for the spotlight by developing products that give an edge in competition and draw the market's attention.

6 Design Validation

Testing of the damper was carried out to validate the design in real world conditions. This chapter describes the approach taken to field validation and presents results describing suspension dynamics in a bottom-out scenario with and without the device. The simulation developed previously is also used to predict a response when parameters match the final prototype damper.

6.1 Methodology for Field Testing

To validate the design, it is important to enact a realistic scenario that creates conditions where the bottom-out damper is required. At the same time the scientific method demands that test conditions are repeatable, and variables can be controlled to yield significant results. This section describes the approach to validating the design on a mountain bike to meet these objectives.

6.1.1 Test site

A safe location was required to carry out field testing where repeated attempts could be carried out with minimum uncertainty. A small drop off a retaining wall beside an unused a bitumen road was selected. A photo of the site is shown in figure 33. This location allowed the rider to pilot the mountain bike over the drop at the same position and speed each trial. The hard impact surface (bitumen road) ensured constant and negligible damping from the ground surface on impact. The vertical drop was 0.6 m and the ground angle at the base 2% downwards in direction of travel. The air spring of the suspension was set at 50 psi so that the fork would reach near full compression when the bike (without damper) landed the drop.

Figure 33: Test site

6.1.2 Data Acquisition

Video analysis was used to track the suspension displacement when the bike travelled over the drop. A GoPro 4 camera was fixed on bicycle frame and recorded at a sampling rate of 240 Hz (frames per second). This was a cost-effective method compared to displacement transducers offering an equivalent sampling rate. Video tracking was also preferable to accelerometers for data acquisition as it is less susceptible to noise and does not introduce integration error (displacement is of primary interest). The camera set-up is shown in figure 34.

Figure 34: Camera set-up

6.1.3 Data Processing

There were several steps involved in retrieving displacement data from video format. These are summarised in figure 35. Tracker software was employed for video analysis using the following procedure:

1. The image was corrected for radial distortion due to the fisheye lens.
2. The image was corrected for perspective distortion due to the viewing angle.
3. A scale was added using a known measurement and axis were aligned on the image.
4. The region to track was defined and auto tracking was run.
5. The video auto tracking results were reviewed.
6. Tabulated displacement, velocity and acceleration data was exported.
7. The time of impact was synchronised across all sets of data for comparison.

Figure 35: Data processing

6.1.4 Bicycle Settings

The prototype bottom-out damper was installed on a Rockshox Lyrik air-sprung mountain bike fork. The dial on the Rockshox damper body allows twelve settings of bottom-out adjustment. The damper adjustment adds preload to the shim stack, restricting fluid flow to increase the damping force. The damper was tested at each quarter (three 'clicks') of the adjustment range. Table 9 describes the suspension and tyre settings used in field validation.

Table 9: Test rig specifications

Setting	Value
Fork Travel	160 mm
Fork spring air pressure	50 psi
Fork low speed compression	2 clicks*
Fork rebound	8 clicks*
Damper suspension fluid	Castrol 10 Wt
Damper air pressure (gas chamber)	25 psi
Bottom-out setting	0, 3, 6, 9, 12 clicks*
Front tyre pressure	30 psi

* clicks of adjustment are counted from the anticlockwise position by convention.

6.1.5 Test Cases

Field testing was carried out for six different cases described in table 10. Video analysis used for data acquisition also allowed speed, position and rider input to be compared across tests to check for consistency. For each case, at least three consistent trials were carried out.

Table 10: Test cases

Case	BOD Adjustment	BOD Damping Force
1 (control)	NA	Zero
2	0 clicks (open)	Minimum
3	3 clicks	Quarter
4	6 clicks	Half
5	9 clicks	Threequarter
6	12 clicks (closed)	Maximum

6.1.6 Evaluation of results

The criteria for analysis follows that discussed for the simulation results in section 4.1.5. The objective of the bottom-out damper is to prevent full compression events without compromising comfort or control. Variables of interest include:

- maximum compression (travel used);
- maximum extension after the impact;
- velocities in compression and rebound;
- accelerations in compression and rebound; and,
- settling time from impact until displacement returns to equilibrium.

6.2 Simulation of the prototype damper

The simulation was adapted for parameters of the prototype damper and test fork to predict results in the field. Displacement results for the simulated prototype design are shown in figure 36. The results predict a 6% decrease in the maximum compression and that full extension can be prevented compared to a standard fork. The settling time is reduced by approximately 18%. The natural frequency and damping ratio are compared to experimental values in the results. The equivalent damping coefficient for the system with the bottom-out damper is predicted to be 644 Ns/m.

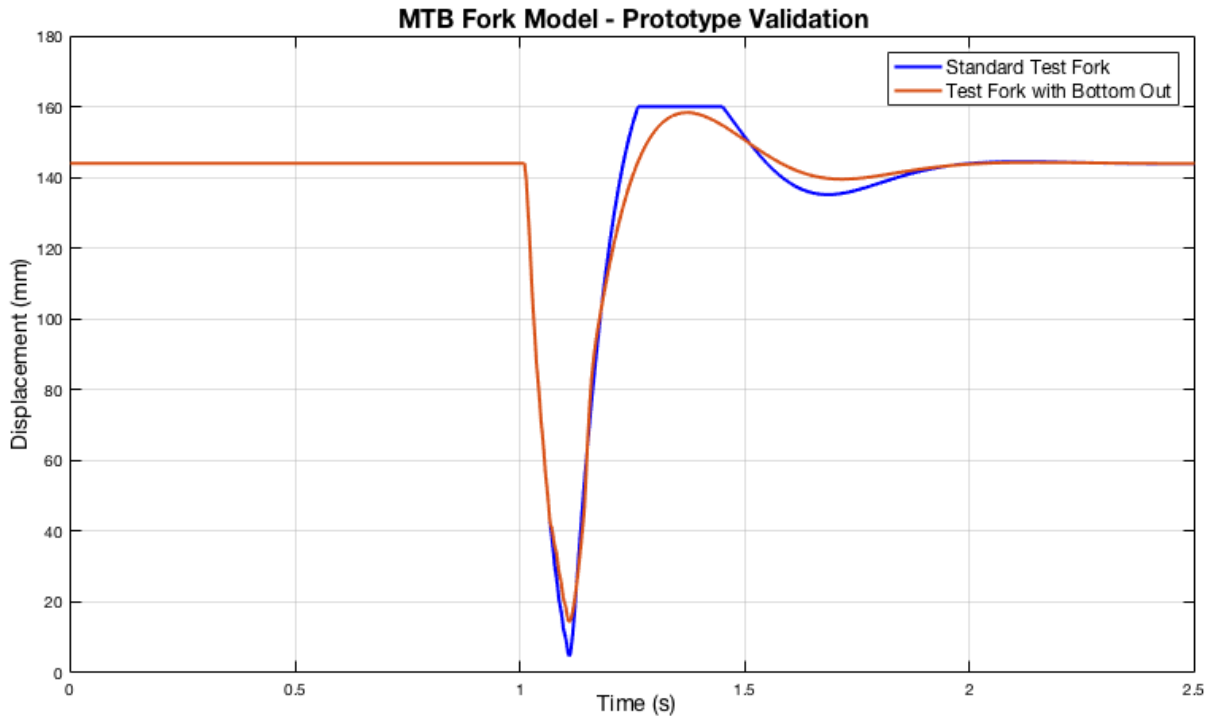

Figure 36: Simulation of prototype design

6.3 Field Validation Results

Results were compiled from the average across three consistent tests for each case. They are presented below for the two extreme cases: without bottom-out damper (No BOD) and with the damper in closed position (BOD Closed). Results for remaining cases (intermediate adjustments of the damper) are included in appendix I. As predicted, these intermediate settings demonstrate moderate results to those included in this section. The results for fork travel are shown as a displacement-time plot in figure 37. The 'BOD Open' case, when the damper is used at the minimum damping setting, is included to demonstrate the range of adjustment.

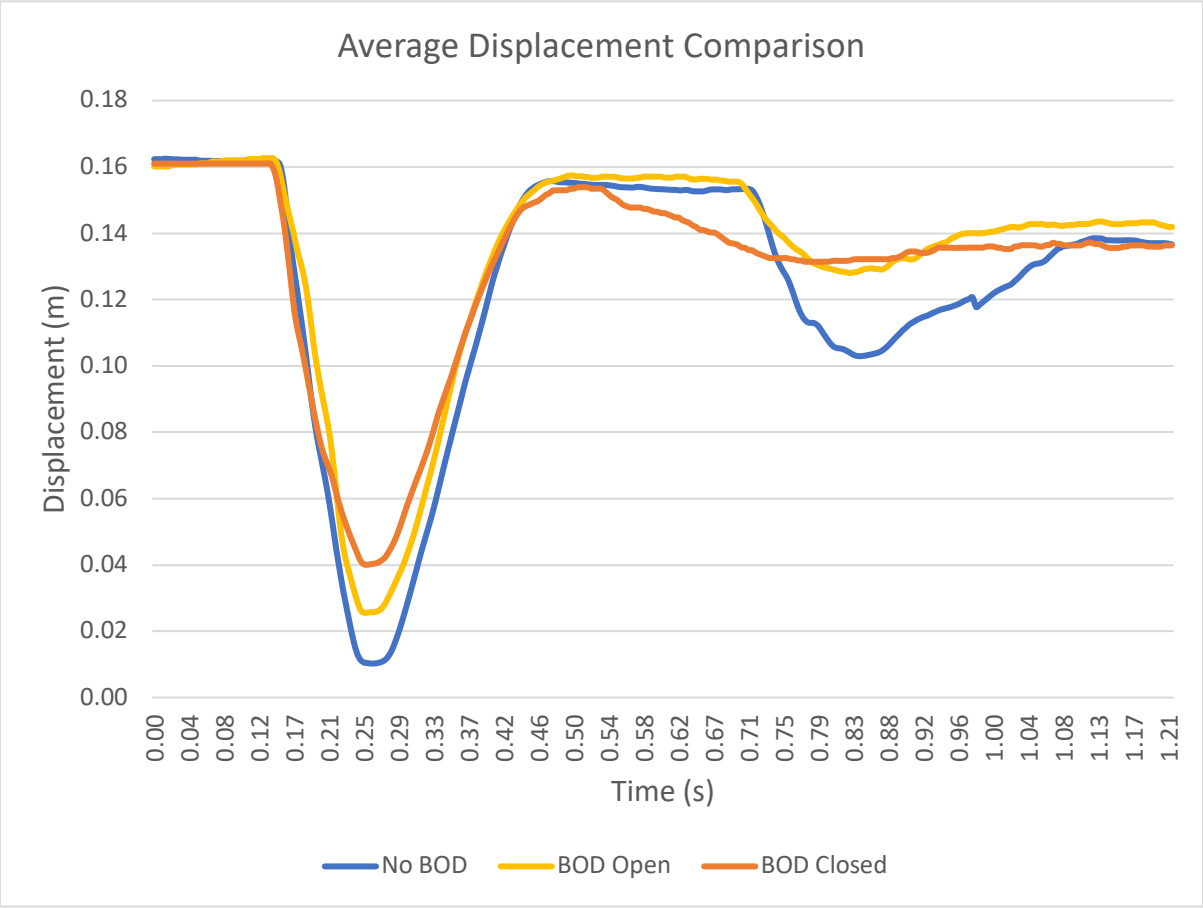

Figure 37: Displacement results

For each case, displacement is initially at full extension (160 mm) when the wheel is in the air before landing. The bottom-out damper reduces maximum compression of the suspension when landing the drop and decreases the settling time for displacement to return to equilibrium. For the closed position (similarly for three quarters closed), the bottom-out damper also prevents a period of full extension following rebound from the impact.

Figure 38 shows the average velocity-time results with and without the bottom-out damper. Generally, lower peak velocities are evident for the damper. Variation in damping between the two cases can be directly implied from velocity results, which is included in the results summary table.

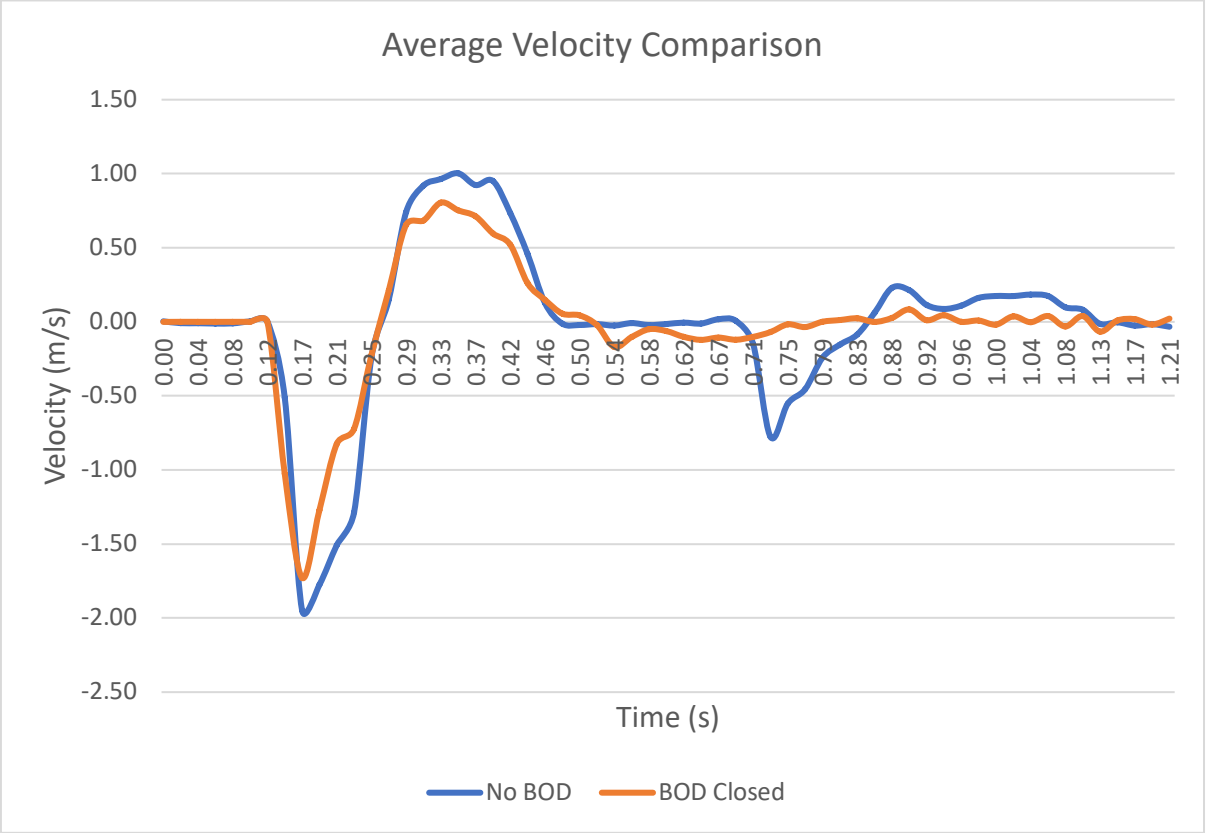

Figure 38: Velocity results

Figure 39 shows results for average acceleration versus time. Similarly, lower peak accelerations are recorded when the bottom-out damper is used. Generally, there is less variation in both velocity and acceleration when the damper is used. A lower variation in normal force can also be implied from the acceleration results.

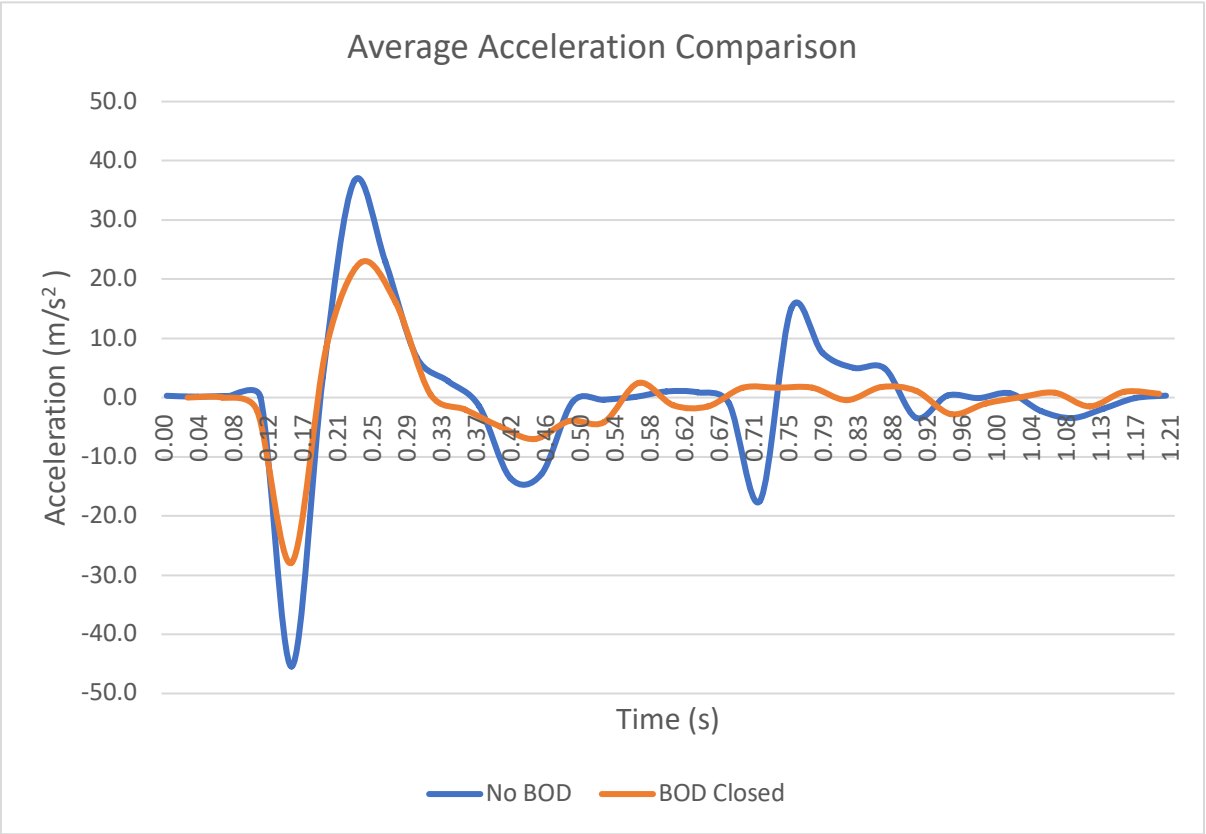

Figure 39: Acceleration results

6.3.1 Summary of results

Table 11 summarises results of interest for quantifying the front suspension performance with the prototype damper. Where possible, test results are also compared to those predicted from the simulation on a relative basis (by the difference when using the damper).

Table 11: Prototype validation results

	No BOD	BOD Closed	Actual Change	Predicted Change
Maximum compression (mm)	150	120	-20%	*-6%*
Maximum extension after impact (mm)	157	154	-2%	*-1%*
Time at full extension (s)	0.24	0	-0.24 s	*- 0.19 s*
Settling time from impact (s)	0.95	0.69	-27%	*-18%*
Peak compression velocity (m/s)	-1.95	-1.73	-11%	
Peak rebound velocity (m/s)	0.92	0.75	-18%	
Relative compression damping	1	1.13	13%	
Relative rebound damping	1	1.23	23%	
Average absolute acceleration (m/s^2)	11.4	9.40	-18%	
Peak absolute acceleration (m/s^2)	45.4	27.9	-39%	
Variation in normal force (standard deviation of average acceleration, m/s^2)	12.3	8.15	-34%	

The force due to the impact is approximately equal for each case in testing. Therefore, the relative damping may be approximated as:

$$Relative\ damping = \frac{b_i}{b_1} = \frac{Fv_{1,peak}}{Fv_{i,peak}} = \frac{v_{1,peak}}{v_{i,peak}} \quad (12)$$

Variation in normal force is quantified using the standard deviation across average accelerations for each case:

$$Variation\ in\ Normal\ Force = \sigma_a = \sqrt{\frac{\sum_{i=1}^{n}(a_i - \bar{a})^2}{n-1}} \quad (13)$$

where n is the number of data points and $\bar{a}$ is the mean acceleration.

6.3.2 Damped System Characteristics

Damped system characteristics can be estimated from measurements of the displacement plot from theory and assuming the general solution for an underdamped linear system. These are shown in table 12 and compared to theoretical results from the simulation.

Table 12: Damped system characteristics

Parameter	No BOD	BOD Closed	Simulation (BOD Closed)
Natural frequency (Hz)	1.77	2.13	*1.76*
Damped natural frequency (Hz)	1.72	1.88	*1.67*
Damping Ratio	0.23	0.47	*0.32*
Equivalent damping coefficient c (Ns/m)	465	1145	*644*

The damped natural frequency can be found from:

$$f_d = \frac{1}{t_2 - t_1} \quad (Hz) \tag{14}$$

where $t_2 - t_1$ is the time between successive compressions.

The damping ratio can be found from the logarithmic decrement δ as:

$$\zeta = \frac{\delta/2\pi}{\sqrt{1+\left(\frac{\delta}{2\pi}\right)^2}} \tag{15}$$

where $\delta = \ln\left(\frac{x_1}{x_2}\right)$,the natural log of the ratio of amplitudes from successive peaks.

The natural frequency can then be calculated as:

$$f_n = \frac{f_d}{\sqrt{1-\zeta^2}} \quad (Hz) \tag{16}$$

The equivalent damping coefficient can be estimated from:

$$c_{eq} = 2\pi * 2m\zeta f_n \quad (Ns/m) \tag{17}$$

where m = 91 kg (mass of rider and bike).

6.4 Uncertainty in Results

An analysis of uncertainty associated with results from field validation was critical to confirm their significance. A large number of potential sources of uncertainty were identified in the testing procedure. These include:

- variations in rider input;
- variations in the velocity and position of bike;
- movement of the camera mount;
- unaccounted distortion from the camera lens;
- measurement error in data processing;
- variations in spring air pressure between tests; and,
- changing friction force between tests due to varying lubrication.

The field validation method was designed in such way to minimise and control for any introduced error. Conditions were controlled as far as possible with the available apparatus. Video footage was reviewed for consistency across trials. Outliers were discounted, and results were averaged across several trials. Therefore, it is assumed random errors occurred from a lack of sensitivity in measuring apparatus rather than the experimental apparatus itself in the calculation of likely error. The following uncertainties were assigned to measurements and data processing on this basis. In general, a value of half the smallest discernible measurement was taken as uncertainty:

- suspension fork measurement, ± 0.5 mm;
- image distortion correction, ± 1 mm; and,
- auto tracking, ± 1 mm.

Figure 40 shows the displacement results from validation presented with band width equivalent to the likely range of uncertainty. All other results were derived from this displacement data.

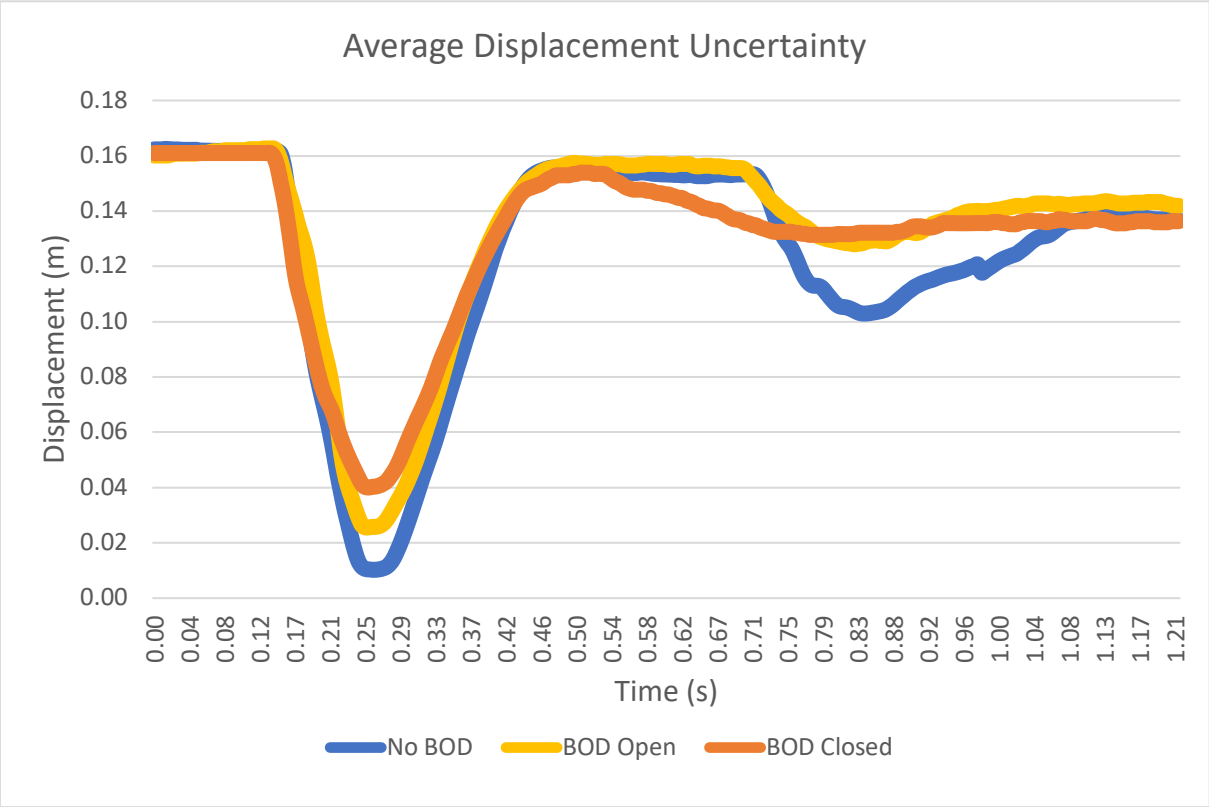

Figure 40: Displacement uncertainty

These displacement results clearly remain significant throughout the range of possible uncertainties. The damper reduces displacement and settling time while improving stability. By extension, any error carried through to average velocity and acceleration calculations does not invalidate key results. It is also possible that systematic errors were present due to flaws in the apparatus such as unaccounted image distortion and limitations of the video analysis software. It is highly probable such error would introduce a consistent bias across the results. For example, full extension after the impact appears slightly less than that before the impact across all cases. In this scenario, relative results between the damper and standard fork maintain their significance and validation results can be reported with confidence.

7 Discussion and Conclusions

The final chapter interprets results from field validation of the bottom-out damper design. Conclusions are drawn with reference to the overall aims of this design project. Recommendations are made for further development of the design, additional validation and potential production of the bottom-out damper.

7.1 Discussion of Results

This section discusses results from validation of the damper design and their implications for performance in downhill mountain bike racing.

7.1.1 Preventing bottom-out and improving control

For the impact tested, the bottom-out damper reduced the maximum compression displacement of the suspension fork by up to 20% (30mm). The level of adjustment on the damper determined the extent of this reduction. The simulation predicted similar displacement results but to a lesser extent (6% reduction). This is likely due to the incorrect assumptions made in the model, particularly underestimation of the damping coefficient. The results demonstrate the design is effective in decreasing the likelihood of a full compression event for a given impact typically experienced over a downhill mountain biking course. This would reduce the overall energy transmitted to the rider and components, improving both comfort and control.

The rebound behaviour of the suspension fork is also influenced by the bottom-out damper. In the closed setting, the damper prevented the fork overshooting to full extension. Without the damper, the test rider reported that the front wheel would ‘bounce’, leaving the ground after landing the drop when the suspension fork extended. This is reflected in results by the flat line at near full extension after the impact for No BOD and Open BOD results. The fork remains extended for approximately 0.24 seconds before the tyre returns to the ground and the suspension can move back towards equilibrium. This equates to an equivalent time without any front wheel traction since there is no normal force between tyre and ground without contact. In racing, this brief loss of traction can quickly lead to loss of control of the

bicycle. In particular, control is desirable as soon as possible after a large impact, such as a drop, to adjust the course of the bike.

The velocity results clearly reveal the damper influences much of the dynamic behaviour of the fork. With the damper, the maximum velocity in compression was reduced by 11% (0.22 m/s) and in rebound by 18% (0.17 m/s). As a result, the equivalent damping constant was 13% higher in compression when using the damper. It is probably that a portion of this increase in perceived damping is a result of additional friction introduced by the design. Specifically, the damper involves two sliding parts: the plunging piston in the fork leg, and the internal floating piston in the damper body. As the fork compresses towards its limit these components move in contact with the fork and damper body, generating a resistive friction force. Unlike the simulated response, it is not clear from results exactly when the bottom-out damper engages. Correlating velocity and displacement results suggests the design adds damping force in a smooth transition from a displacement as large as 100 mm. This gradual transition to increased damping ensures more predictable suspension performance for the rider.

An additional consequence of the higher damping is the reduced settling time for the fork to return to equilibrium. Settling time is reduced by 27% compared to a standard fork and a predicted 18% reduction. This presents another control advantage of using the bottom-out damper. A faster return to equilibrium means the fork and rider can respond to a subsequent impact sooner, without any influence from the earlier bump.

7.1.2 Reducing accelerations for more comfort and traction

When the damper was used, peak accelerations of the suspension fork decreased by up to 39%. Similarly, average accelerations reduced by 18% from 11.4 m/s^2 without the BOD. These lower accelerations may improve the comfort of the rider by preventing the transfer of vibrations. It also allows them more time to react to changes in the suspension motion and corresponding changes in the geometry of the bike. However, the initially lower accelerations may indicate the suspension with the bottom-out damper cannot react as quickly to changes in terrain. This could be a result of increased unsprung mass and inertia, or greater friction when the damper is present. Also of interest is the variation in fork accelerations, which is

directly proportional to variation in the normal force and by consequence, inversely proportional to traction with the ground. The standard deviation of the acceleration was used as a metric for this variability (note that 68% of values lie within one standard deviation of the mean for a normal distribution). With this measure, test results show a 34% decrease in the variation of the normal force when the damper is used. Therefore, the damper improves traction which enhances control of a mountain bike over rough terrain.

7.1.3 Better damping characteristics for racing

Calculation of damped system properties from the displacement response helps to explain the large change in dynamics described above. The damper increased the equivalent damping coefficient for the fork from 465 to 1145 Ns/m, compared to 644 Ns/m predicted. This reaffirms the calculation of damping coefficient from geometry was inaccurate and highlights the challenges of correctly applying theory to damper design. The validation results indicate that the bottom-out damper doubled the damping ratio of the response from 0.23 to 0.47. This difference is strikingly similar to automotive suspension applications, passenger vehicles have a damping ratio around 0.2 compared to 0.5 or more for off-road rally vehicles. A higher damping ratio is evidently desirable for high speed control across all kinds of disciplines including mountain biking.

7.2 Conclusions

Downhill mountain bike racing is an extreme sport that pushes both rider and components to their limit. This design project has focussed on improving one aspect of what is arguably the most important and complex mechanical system found on a bike, the suspension. Specifically, there was need to control the front suspension bottom-out: when full compression of the suspension causes harsh impacts to be transmitted to the rider and components. This project has demonstrated that a damper for the last stage of compression is an effective solution to the bottom-out problem in downhill mountain biking. The concept was first of all proven by simulation of a suspension system comparing different methods to control for bottom-out, including use of stiffer springs or higher damping. When the proposed bottom-out damper was modelled, the suspension response demonstrated the best performance in terms of comfort and control objectives.

The bottom-out damper was designed from existing components and custom manufactured parts, assembled and installed on a mountain bike. Validation of the design was carried out on the mountain bike using video analysis in a controlled testing environment. Results show the damper successful in decreasing the amount of travel used by up to 20% to prevent full compression. The increased damping force provided by the design also improves tyre contact with the ground over time by preventing rebound overshoot and affords better traction by minimising the variation in accelerations. This translates to a more controlled mountain bike and potentially higher speeds in downhill mountain bike racing.

While improvements to the design can be made, the prototype bottom-out damper performed successfully and as intended. There is an opportunity to further develop the current design for production or adopt aspects of the design to improve future mountain bike suspension products. Neither of these can occur without investment from the industry since by its nature the development of suspension products is expensive. Downhill mountain bike racing, as a relatively exclusive sport, has provided the rare opportunity to design something that raises the performance of suspension products above what is currently available.

7.3 Recommendations

With the benefit of hindsight, a number of recommendations are made from experience gained from the project. The bottom-out damper design could be improved by:

- minimising the total weight of the damper by reducing the volume of suspension oil required;
- increasing the range of damping adjustment so that the open position results in a suspension performance similar to a standard fork; and,
- employing advanced analysis techniques such as computational fluid dynamics to optimise the damping mechanism.

For further validation of the design, additional testing should be carried out including:

- testing in a laboratory with a shock dynamometer to generate more results with more detail and precision;
- extending data acquisition and analysis over the full course of a mountain bike trail;
- gaining elite rider feedback after extended use of the design;
- varying additional damper settings including suspension oil viscosity, air pressure and shim stack configuration to determine optimal set up of the damper; and,
- quantifying the time advantages that the damper offers over a typical trail.

Insights were gleaned through the design process that may contribute to the development of future mountain bike suspension. These include:

- the suspension system can be discretised into smaller subsystems but modifying the design of these should consider how subsystems interact to achieve overall performance objectives for mountain biking;
- efforts to improve suspension performance should focus on providing greater control over damping; and,
- position sensitive damping or active suspension designs provide an avenue for the future progression of mountain bike suspension.

8 References:

Bauer, W., 2011. *Hydropneumatic Suspension Systems*, Berlin, Heidelberg: Springer Berlin.

Croccolo, D., De Agostinis, M. & SpringerLink Content Provider., 2013. *Motorbike Suspensions Modern design and optimisation*, London: Springer London: Imprint: Springer.

Davie, M., 2011. *Mountain bike suspension systems and their effect on rider performance quantified through mechanical, psychological and physiological responses*. pp.PQDT - UK & Ireland.

Dixon, C., 2007. *The Shock Absorber Handbook*, London: Wiley-Blackwell.

Els, P., Theron, N., Uys, P. & Thoresson, M., 2007. The ride comfort vs. handling compromise for off-road vehicles. *Journal of Terramechanics*, 44(4), pp.303–317.

Ericksen, E., Cox, C. & Perlot, S., 2012. *Methods and Apparatus for Position Sensitive Damping*. Patent.

Grether, W., 1971. Vibration and human performance. *Human factors*. 13. 203-16. doi:10.1177/001872087101300301.

Hurst, H., Swarén, M., Hébert-Losier, K., Ericsson, F., Sinclair, J., Atkins, S., & Holmberg, H., 2012. Influence of course type on upper body muscle activity in elite Cross-Country and Downhill mountain bikers during off Road Downhill Cycling. *Journal of Science And Cycling*, 1(2), pp.2-9.

Ishii, T., Umemura, Y., Kitagawa, K., 2003. Influences of mountain bike suspension systems on energy supply and performance. *Japanese Journal of Biomechanics in Sports and Exercise*, 7(1), pp. 2-9.

Jiang, X., Wang, J. & Hu, H., 2012. Semi-active control of a vehicle suspension using magneto-rheological damper. *Journal of Central South University*, 19(7), pp.1839–1845.

Jianmin, G., Gall, R. & Zuomin, W., (*2001*). Dynamic Damping and Stiffness Characteristics of the Rolling Tire. *Tire Science and Technology*, 29(4), pp. 258-268.

Kasprzak, J., 2014. *Understanding your Dampers: A guide from Jim Kasprzak*. [online] Kaz Technologies. Available at: http://www.kaztechnologies.com/wp-

content/uploads/2014/03/A-Guide-To-Your-Dampers-Chapter-from-FSAE-Book-by-Jim-Kasprzak.pdf [Accessed 26 Oct. 2017].

Laser, M. & Bauer, T, 1997., The effects of selected mountain bike front suspension forks on handlebar vibration and ground reaction forces. *ProQuest Dissertations and Theses*.

Levy, M. & Smith, G., 2005. Effectiveness of vibration damping with bicycle suspension systems. *Sports Engineering*, 8(2), pp.99–106.

Macdermid, P., 2015. Ergonomic Interventions, Health and Injury Prevention during Off-Road Mountain Biking. *Journal of Ergonomics* 5: e130. doi: 10.4172/2165-7556.1000e130

MacRae, H.S.-H., Hise, K.J. & Allen, P., 2000. Effects of front and dual suspension mountain bike systems on uphill cycling performance. *Medicine & Science in Sports & Exercise*, 32(7), pp.1276–1280.

Miller, M., Macdermid, P., Fink, P Stephen, S. & Stannard, S., 2017 Performance and physiological effects of different descending strategies for cross-country mountain biking. *European Journal of Sport Science* 17:3, pp. 279-285.

Nakamura, H. & Haverkamp, M., 1991. Effects of whole-body vertical shock-type vibration on human ability for fine manual control. *Ergonomics*, 34(11), pp.1365–1376.

Nielens, H. & Lejeune, T., 2004. Bicycle Shock Absorption Systems and Energy Expended by the Cyclist. *Sports Medicine*, 34(2), pp.71–80.

Orendurff, M.S., Fujimoto, K. & Smith, G.A., 1994. The effect of mountain bike suspension fork stiffness on impact acceleration characteristics. *Medicine & Science in Sports & Exercise*, 26(Supplement), p.S176.

Pinkbike, 2017. *Mountain bike news, photos, videos and events - Pinkbike*. [online] Pinkbike.com. Available at: https://www.pinkbike.com [Accessed 26 Oct. 2017].

Race Only Springs, 2017. *Spring Tech Specs | Race Only Springs*. [online] Raceonlysprings.com. Available at: https://www.raceonlysprings.com/home/spring-tech-specs/ [Accessed 26 Oct. 2017].

Racetech, 2018. *G3-S Shock Types*. [online] Racetech.com. Available at: http://www.racetech.com/page/title/g3s%20shock%20types [Accessed 26 May 2018].

Rockshox, 2017. *RockShox*. [online] Sram.com. Available at: https://www.sram.com/rockshox [Accessed 26 Oct. 2017].

Schobeiri, M., 2014. *Fluid Mechanics for Engineers.* Berlin: Springer Berlin.

Shiao, Y.J. & Nguyen, T.S., 2015. Using magnetorheological fluids in an innovative hybrid bicycle damper. *IOP Conference Series*: Materials Science and Engineering, 103(1), p.8.

Titlestad, J., Fairlie-Clarke, T., Davie, M., Whittaker & Grant, S., 2003. Experimental Evaluation of Mountain Bike Suspension Systems. *Acta Polytechnica*, 43(5), Acta Polytechnica, 01 January 2003, Vol.43(5).

Yeh, F. & Chen, Y., 2013. Semi-active bicycle suspension fork using adaptive sliding mode control. *Journal of Vibration and Control*, 19(6), pp.834–846.

Appendices

Appendix A – Theoretical Equations

Derivation of 2 DOF Transfer Function

$$M_1\ddot{X}_1 = -c_1(\dot{X}_1 - \dot{X}_2) - K_1(X_1 - X_2)$$
$$M_2\ddot{X}_2 = c_1(\dot{X}_1 - \dot{X}_2) + K_1(X_1 - X_2) + c_2(\dot{W} - \dot{X}_2) + K_2(W - X_2)$$

$$(M_1s^2 + c_1s + K_1)X_1(s) - (c_1s + K_1)X_2(s) = 0$$

$$-(c_1s + K_1)X_1(s) + (M_2s^2 + (c_1 + c_2)s + K_1 + K_2)X_2(s) = (c_2s + K_2)W(s)$$

$$\begin{bmatrix}(M_1s^2 + c_1s + K_1) & -(c_1s + K_1)\\ -(c_1s + K_1) & (M_2s^2 + (c_1 + c_2)s + K_1 + K_2)\end{bmatrix}\begin{bmatrix}X_1(s)\\ X_2(s)\end{bmatrix} = \begin{bmatrix}0\\ (c_2s + K_2)W(s)\end{bmatrix}$$

$$A = \begin{bmatrix}(M_1s^2 + c_1s + K_1) & -(c_1s + K_1)\\ -(c_1s + K_1) & (M_2s^2 + (c_1 + c_2)s + K_1 + K_2)\end{bmatrix}$$

$$\Delta = det\begin{bmatrix}(M_1s^2 + c_1s + K_1) & -(c_1s + K_1)\\ -(c_1s + K_1) & (M_2s^2 + (c_1 + c_2)s + K_1 + K_2)\end{bmatrix}$$

$$= (M_1s^2 + c_1s + K_1)\cdot(M_2s^2 + (c_1 + c)s + K_1 + K_2) - (c_1s + K_1)^2$$

$$\begin{bmatrix}X_1(s)\\ X_2(s)\end{bmatrix} = A^{-1}\begin{bmatrix}0\\ (c_2s + K_2)W(s)\end{bmatrix}$$

$$\begin{bmatrix}X_1(s)\\ X_2(s)\end{bmatrix} = \frac{1}{\Delta}\begin{bmatrix}(M_2s^2 + (c_1 + c_2)s + K_1 + K_2) & (c_1s + K_1)\\ (c_1s + K_1) & (M_1s^2 + c_1s + K_1)\end{bmatrix}\begin{bmatrix}0\\ (c_2s + K_2)W(s)\end{bmatrix}$$

$$= \frac{1}{\Delta}\begin{bmatrix}(M_2s^2 + (c_1 + c_2)s + K_1 + K_2) & (c_1c_2s^2 + (c_1K_2 + c_2K_1)s + K_1K_2)\\ (c_1s + K_1) & (M_1c_2s^3 + (M_1K_1 + c_1c_2)s^2 + (c_1K_2 + c_2K_1)s + K_1K_2)\end{bmatrix}\begin{bmatrix}0\\ W(s)\end{bmatrix}$$

$$G(s) = \frac{X_1(s) - X_2(s)}{W(s)} = \frac{-M_1c_1s^3 - M_1K_2s^2}{\Delta}$$

$$\Delta = M_1M_2s^4 + (c_1(M_1 + M_2) + c_2M_1)s^3 + (c_1c_2 + M_1(K_1 + K_2) + M_2K_1)s^2 + (c_1K_2 + c_2K_1)s + K_1K_2$$

Appendix B – Root Locus Analysis

The root-locus method was used to investigate how the dynamics of the system change when the suspension damping parameter c_1 and spring stiffness parameter k_1 are varied. The open loop equation with damping control and spring stiffness control respectively are:

$$\Delta = M_1M_2s^4 + (c_1(M_1 + M_2) + c_2M_1)s^3 + (c_1c_2 + M_1(K_1 + K_2) + M_2K_1)s^2 + (c_1K_2 + c_2K_1)s + K_1K_2$$

$$R.L.E. = b_1\frac{N(s)}{D(s)} = c_1\frac{(M_1 + M_2)s^3 + c_2s^2 + K_2s}{M_1M_2s^4 + c_2M_1s^3 + (M_1(K_1 + K_2) + M_2K_1)s^2 + c_2K_1s + K_1K_2} = -1$$

$$c_1\frac{95.5s^3 + 70s^2 + 150000s}{409.5s^4 + 6370s^3 + 14480850s^2 + 609000s + 1305000000} = -1$$

$$R.L.E. = K_1\frac{N(s)}{D(s)} = K_1\frac{(M_1+M_2)s^2 + c_2s + K_2}{M_1M_2s^4 + (c_1(M_1 + M_2) + c_2M_1)s^3 + (c_1c_2 + M_1K_2)s^2 + c_1K_2s} = -1$$

$$K_1\frac{95.5s^2 + 70s + 150000}{409.5s^4 + 92320s^3 + 13713000s^2 + 7830000s} = -1$$

The following table describes the poles and transient characteristics for each open loop system defined above:

Damping Gain c_1			
Poles	**Damping**	**Frequency (rad/s)**	**Time constant (s)**
-1.16e-03+9.51i	1.22e-04	9.51	8.61e02
-1.16e-03-9.51i	1.22e-04	9.51	8.61e02
-7.78+1.88e02i	4.14e-02	1.88e02	1.29e-01
-7.78-1.88e02i	4.14e-02	1.88e02	1.29e-01
Spring Stiffness Gain K_1			
Poles	**Damping**	**Frequency (rad/s)**	**Time constant (s)**
0.00	-1.00	0	Inf
-1.06e01	1.00	1.06e+01	9.47e-02
-1.07e02+1.40e02i	6.08e-01	1.77e+02	9.31e-03
-1.07e02-1.40e02i	6.08e-01	1.77e+02	9.31e-03

The root locus shown in figure 41 describes how the closed loop poles move varying c_1 from zero to infinity. The root locus intersects the real axis when damping is critical. Increasing c_1 from the default value of approximately 900 Ns/m causes the dominant pole to move left and towards the real axis. This leads to a suspension response with less oscillations and overshoot.

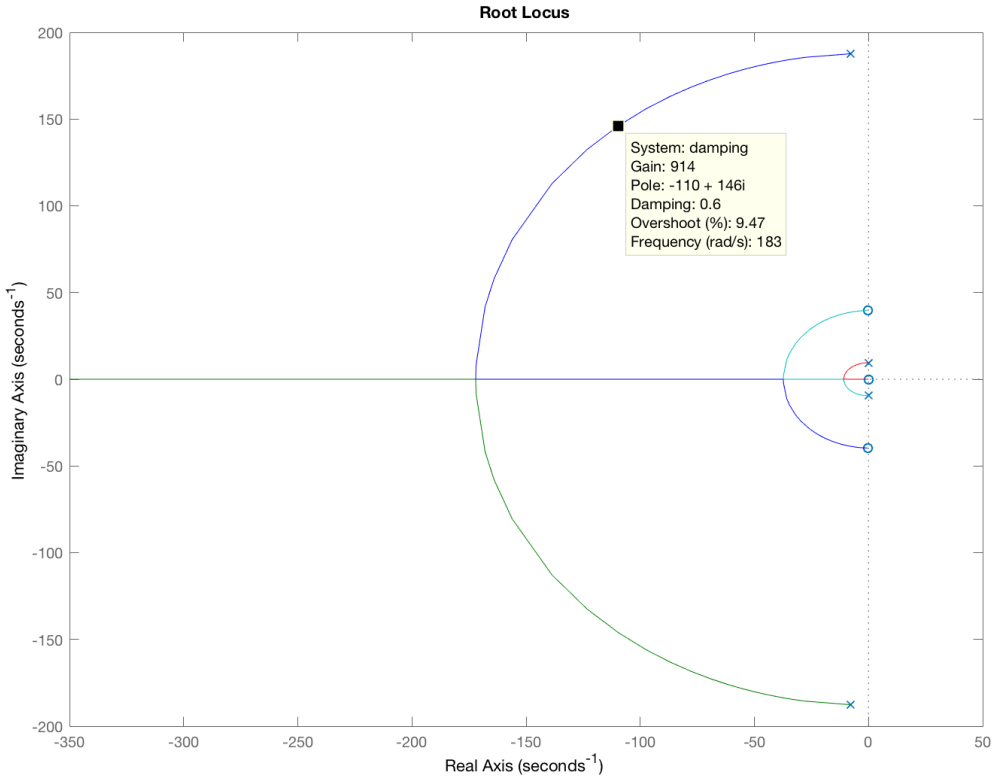

Figure 41: Damping gain root locus

The root locus shown in figure 42 describes how the closed loop poles move varying K_1 from zero to infinity. It demonstrates that increasing K_1 from an initial value of 7800 N/m causes the dominant pole to move right and away from the real axis. This leads to a higher frequency suspension response with more oscillations of a greater amplitude.

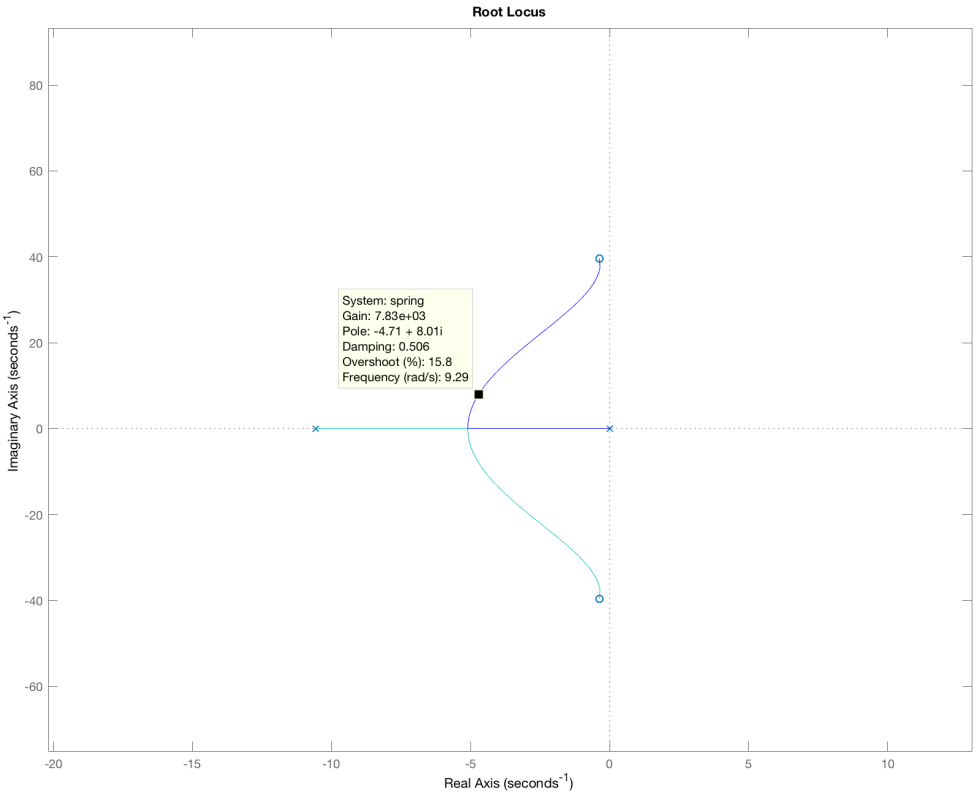

Figure 42: Spring stiffness gain root locus

Matlab Code

```
%Root Locus analysis
damping=tf([m1+m2 c2 k2 0],[m1*m2 c2*m1 m1*(k1+k2)+m2*k1 c2*k1 k1*k2])
damp(damping)
rlocus(damping)

spring=tf([m1+m2 c2 k2],[m1*m2 c1*(m1+m2)+c2*m1 c1*c2+m1*k2 c1*k2 0])
damp(spring)
rlocus(spring)
```

Appendix C – Matlab Code for Simulation and Analysis

Matlab code for simulation and damped analysis

```
%Mountain Bike Suspension Fork Model

clear;
Ms=91; %Sprung mass [kg]
Mu=4.5; %Unsprung mass [kg]
ks=8700; %Suspension spring constant[N/m](8700 def)
ku=150000; %Tyre spring constant[N/m] (150000 def)
cs=900; %Suspension compression damping constant [Ns/m] (900 def)
cu=70; %Tyre damping constant[Ns/m]
h=0.30; %bump height [m] (0.3 def)
bot=5; %Bottom out damping gain [Ns/m] (1 def)
reb=1.2; %rebound damping bias (1.2 def)

%Matrix equation of motion
M=[m1,0;0,m2];
C=[-c1,c1;c1,c1+c2];
K=[-k1,k1;k1,k1+k2];

%Undamped analysis
[P,D]=eig(inv(M)*K);
natfreq1hz=abs(sqrt(diag(D))/2/pi) %natural frequency

%Damped anlysis
[P1,D1]=eig([zeros(2,2),eye(2,2);-inv(M)*K,inv(M)*C]);
dampfreq1hz=abs(imag(diag(D1))/2/pi) %damped natural frequency
dampratio=abs(real(diag(D1))./abs(diag(D1))) %damping ratio


%Transfer Function
num=[-m1*c1 -m1*k2 0 0];
den=[(m1*m2) (c1*(m1+m2)+c2*m1) (c1*c2+m1*(k1+k2)+m2*k1) (c1*k2+c2*k1)
(k1*k2) ];
susp=tf(num,den)
damp(susp) %damped system parameters
rlocus(susp) %plot root locus of transfer function
```

Matlab code for prototype simulation

```
clear;
%Prototype damper parameters
Ms=91; %Sprung mass [kg]
Mu=4.5; %Unsprung mass [kg]
ks=8700; %Suspension spring constant[N/m]
ku=150000; %Tyre spring constant[N/m]
cs=665; %Suspension compression damping constant [Ns/m]
cu=70; %Tyre damping constant[Ns/m]
h=0.23; %bump height [m]
bot=1890/cs; %Bottom out damping gain [Ns/m] =1 when no bottom out damper
reb=1.9; %rebound damping bias
```

Appendix D – Simulink Model Design

MTB Fork Subsystem

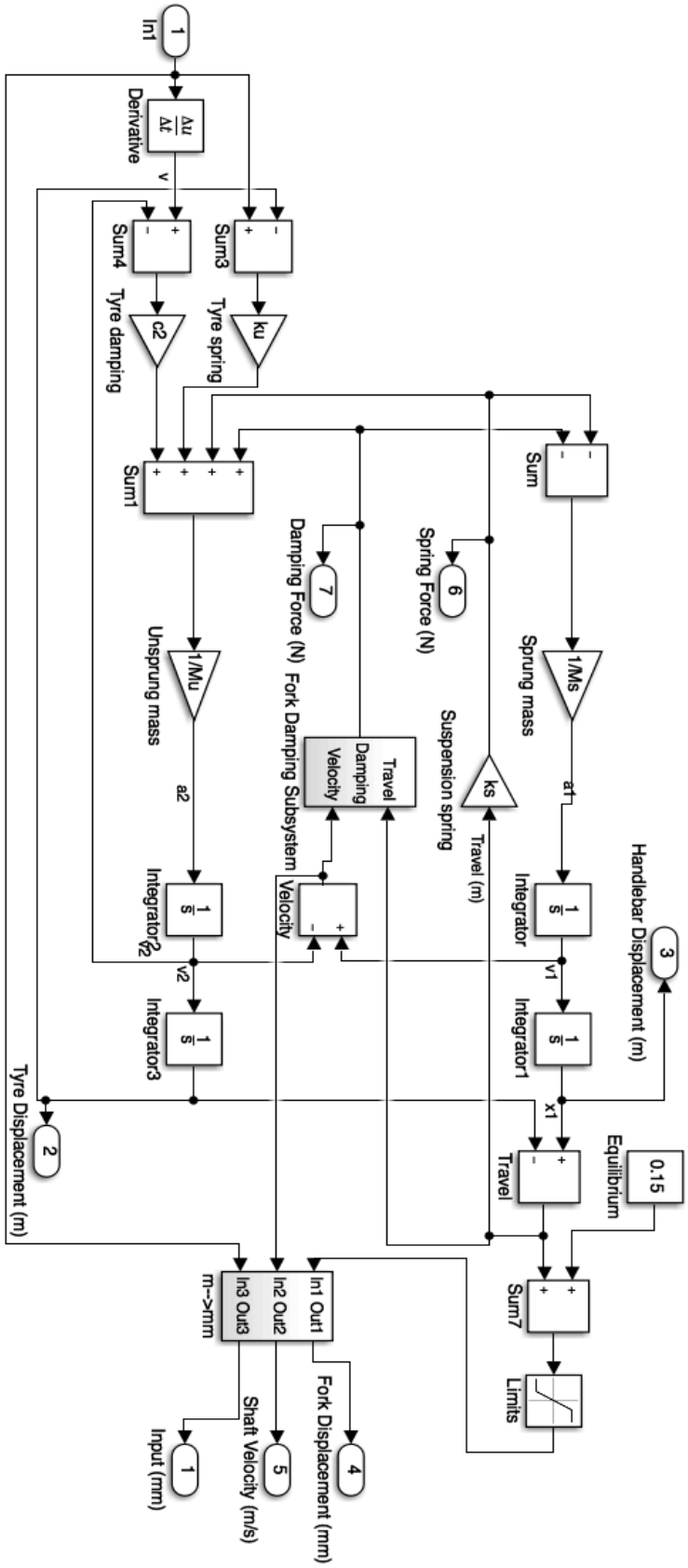

Inputs and outputs

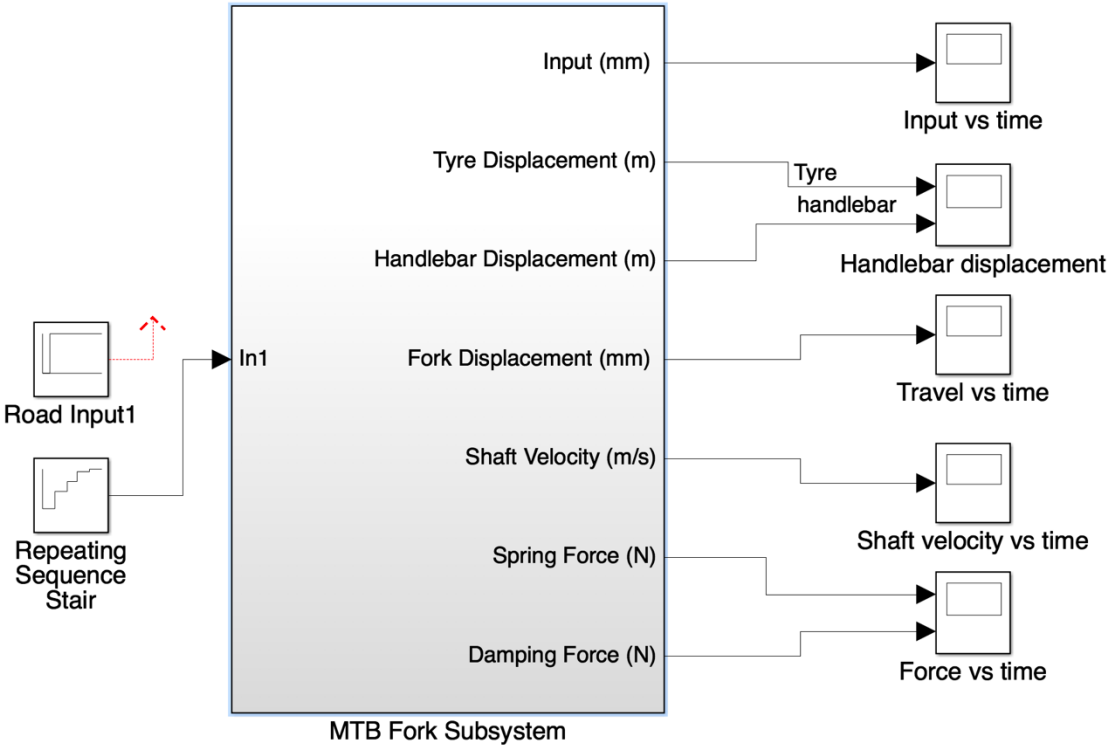

Fork Damping Subsystem

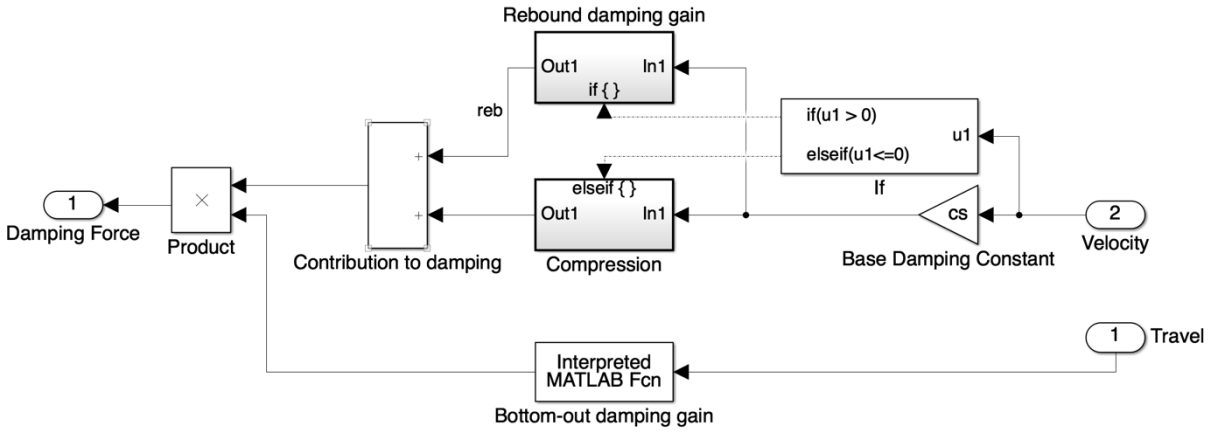

Appendix E – Simulation Results

Single Impact Tyre and Wheel Displacement

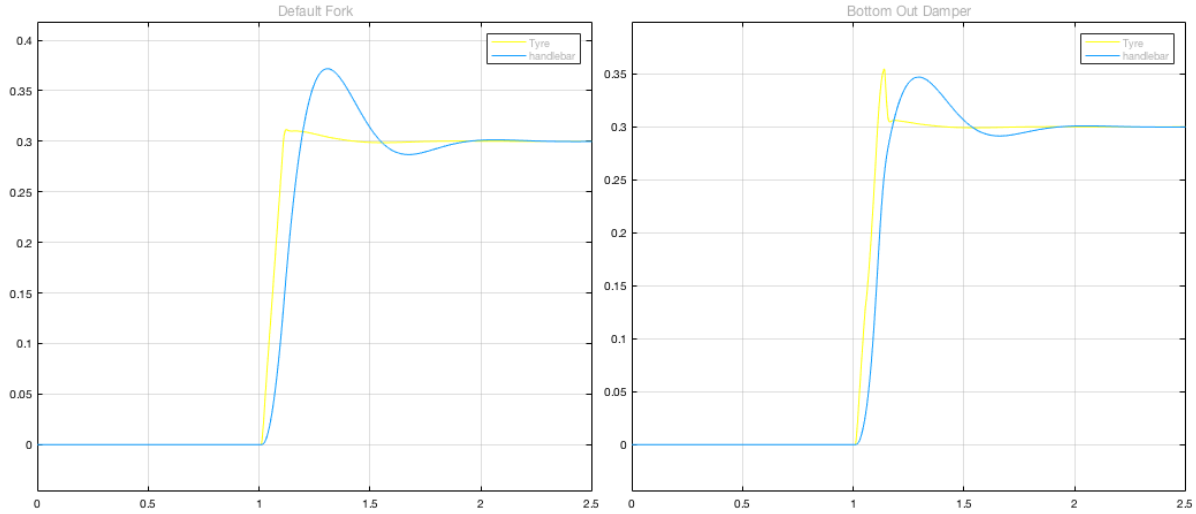

Single Impact Velocity

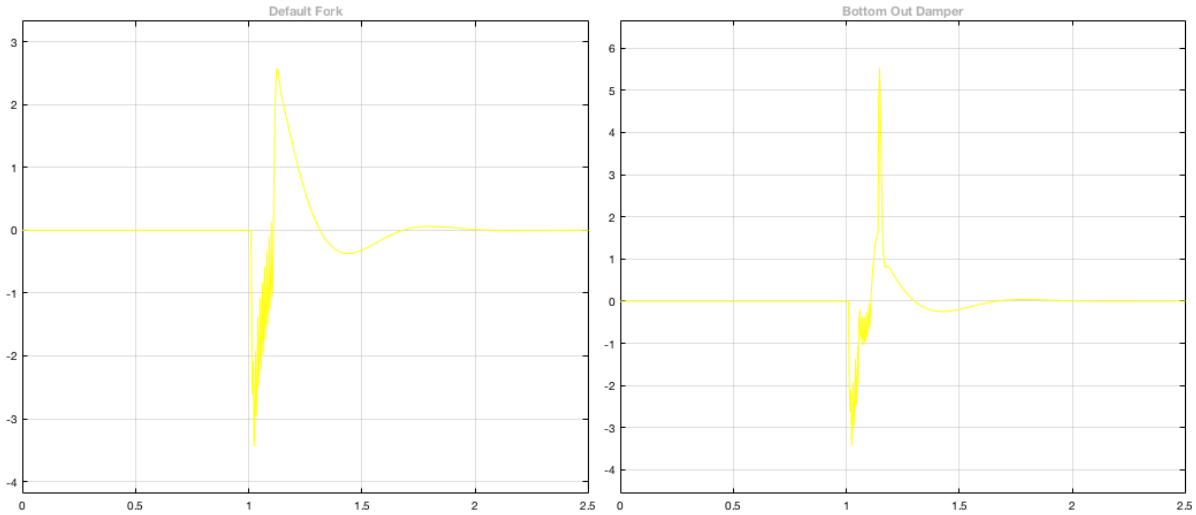

Single Impact Spring and Damping Forces

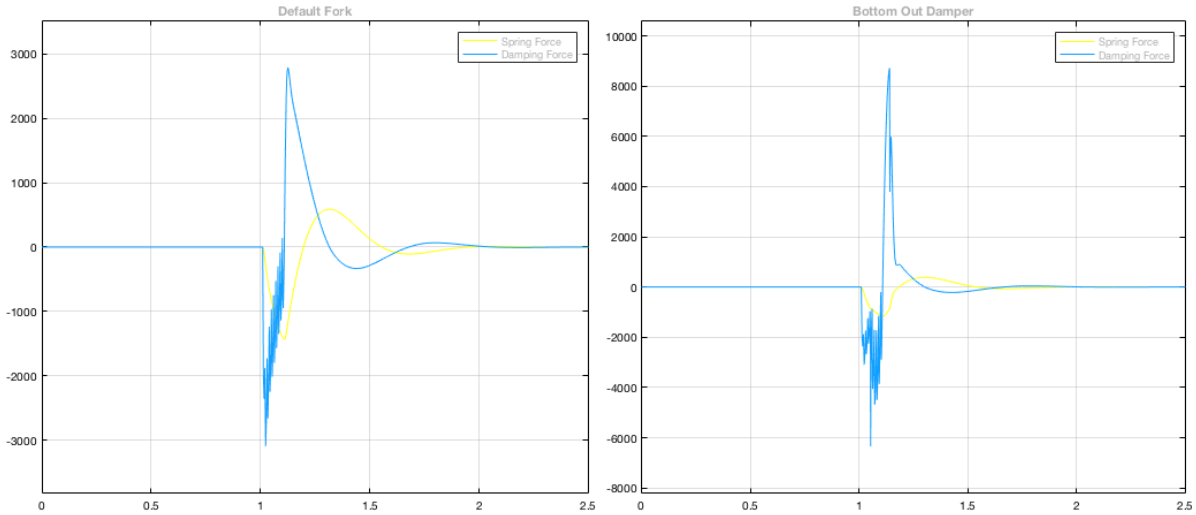

Repeated Impact Displacement

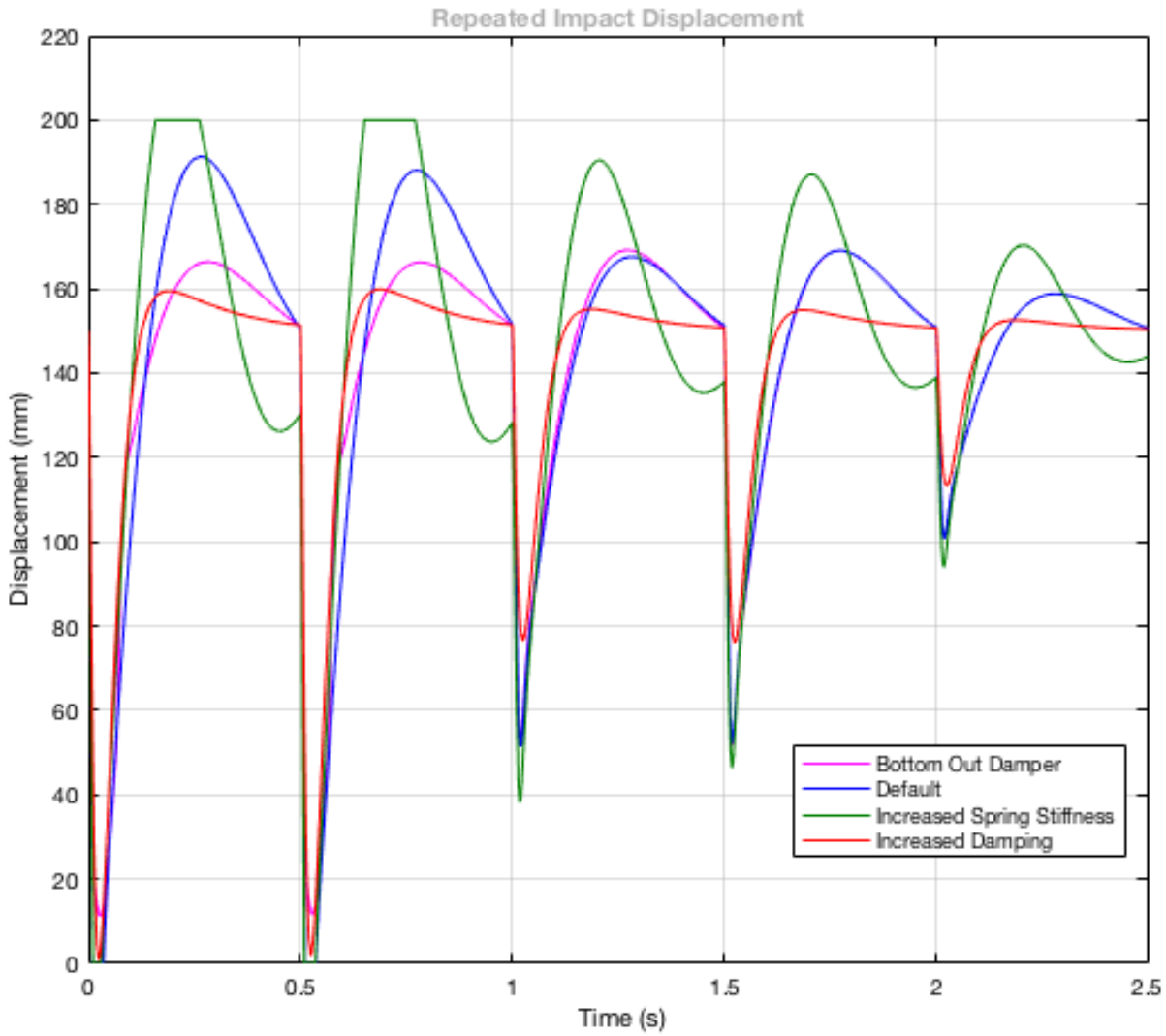

Repeated Impact Wheel and Handlebar Displacement

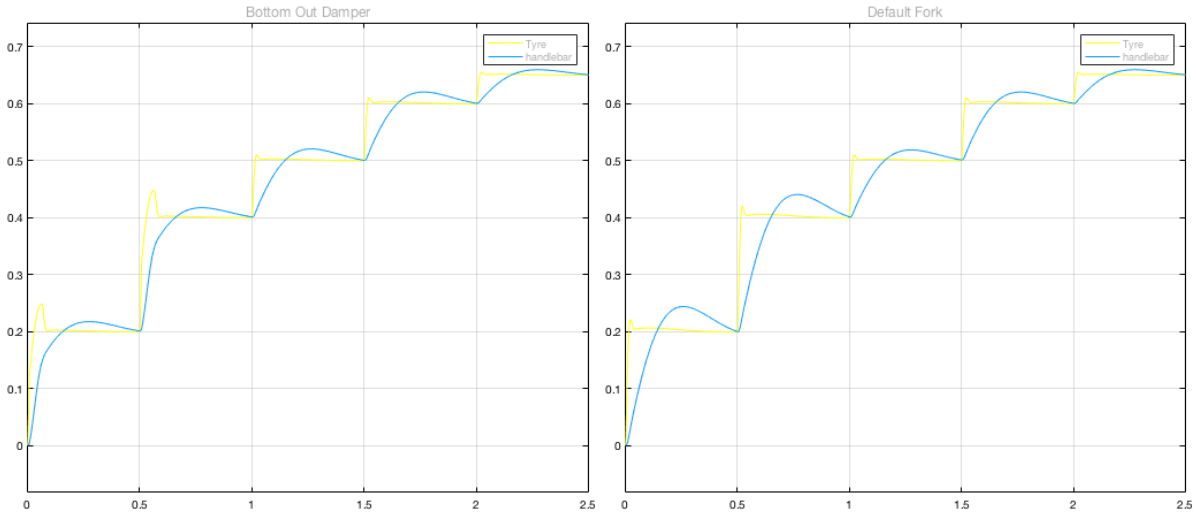

Repeated Impact Velocity

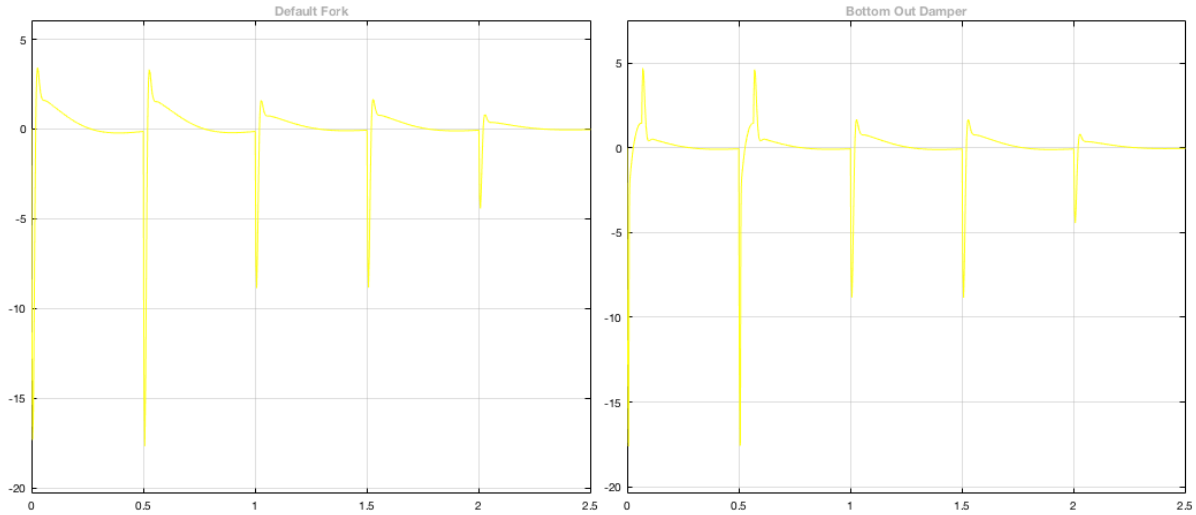

Repeated Impact Spring and Damping Forces

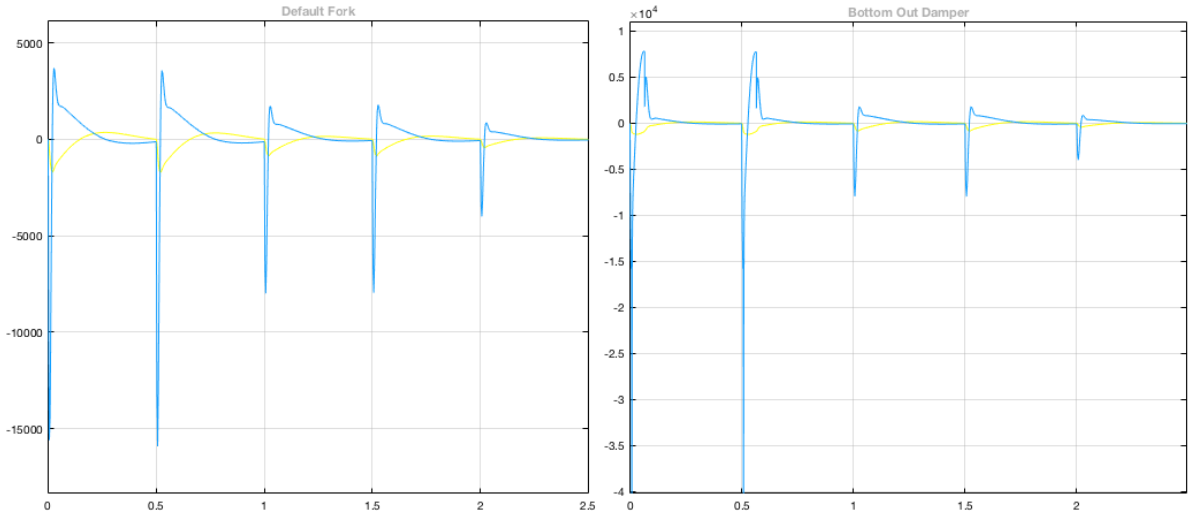

Small Repeated Impacts Displacement

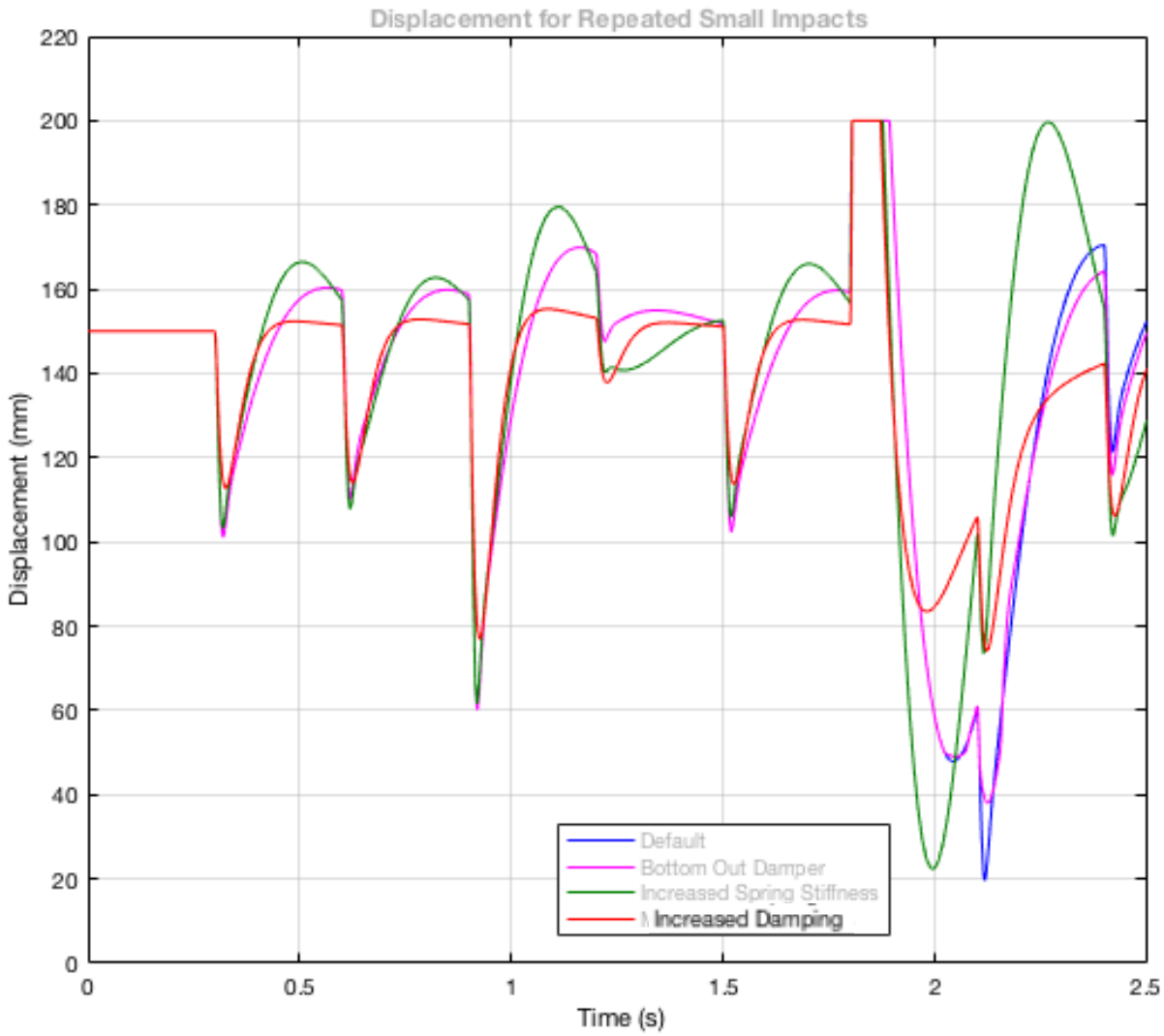

Appendix F – Bottom Plate Drawings

Production Bottom Plate

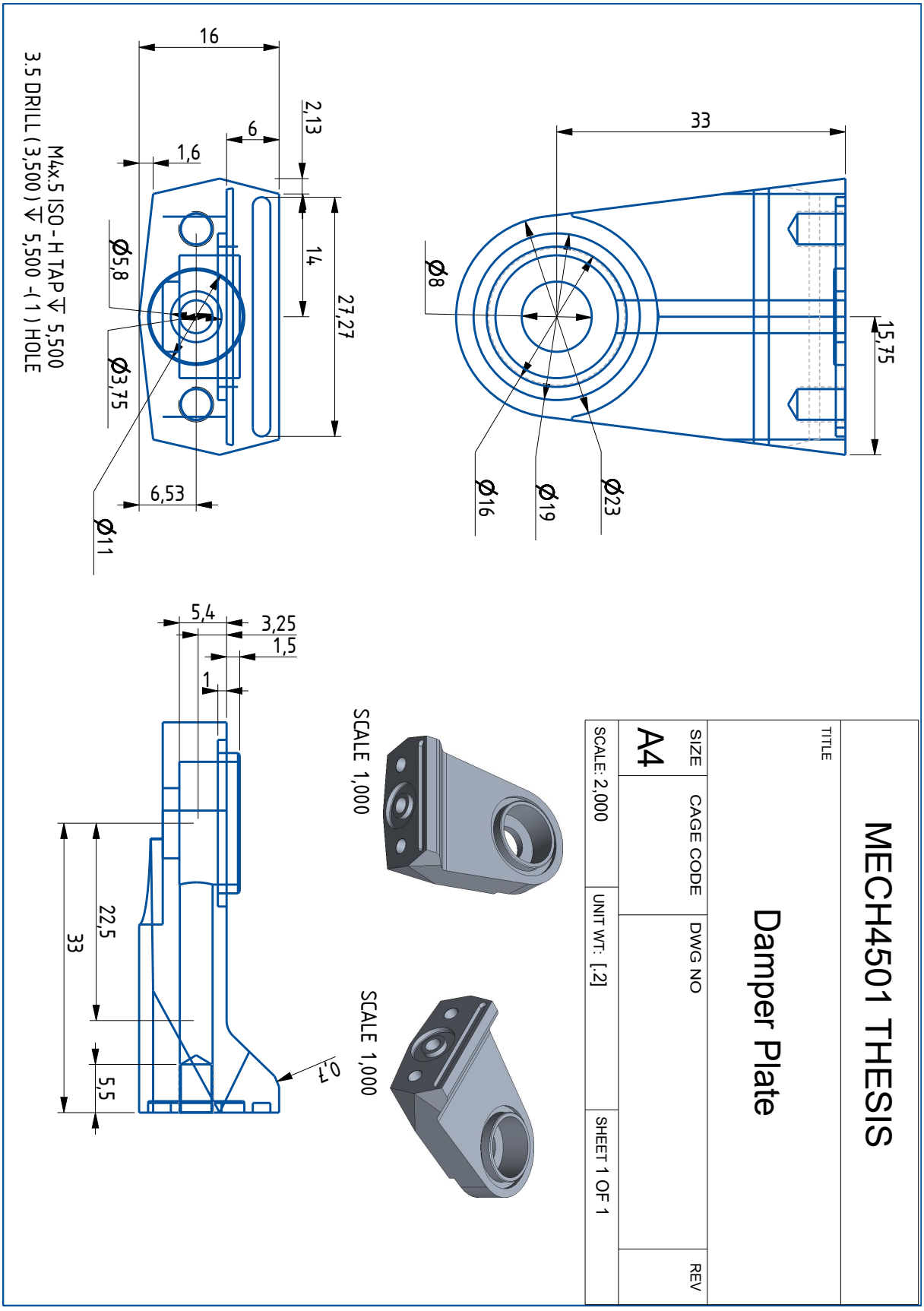

Prototype Bottom Plate

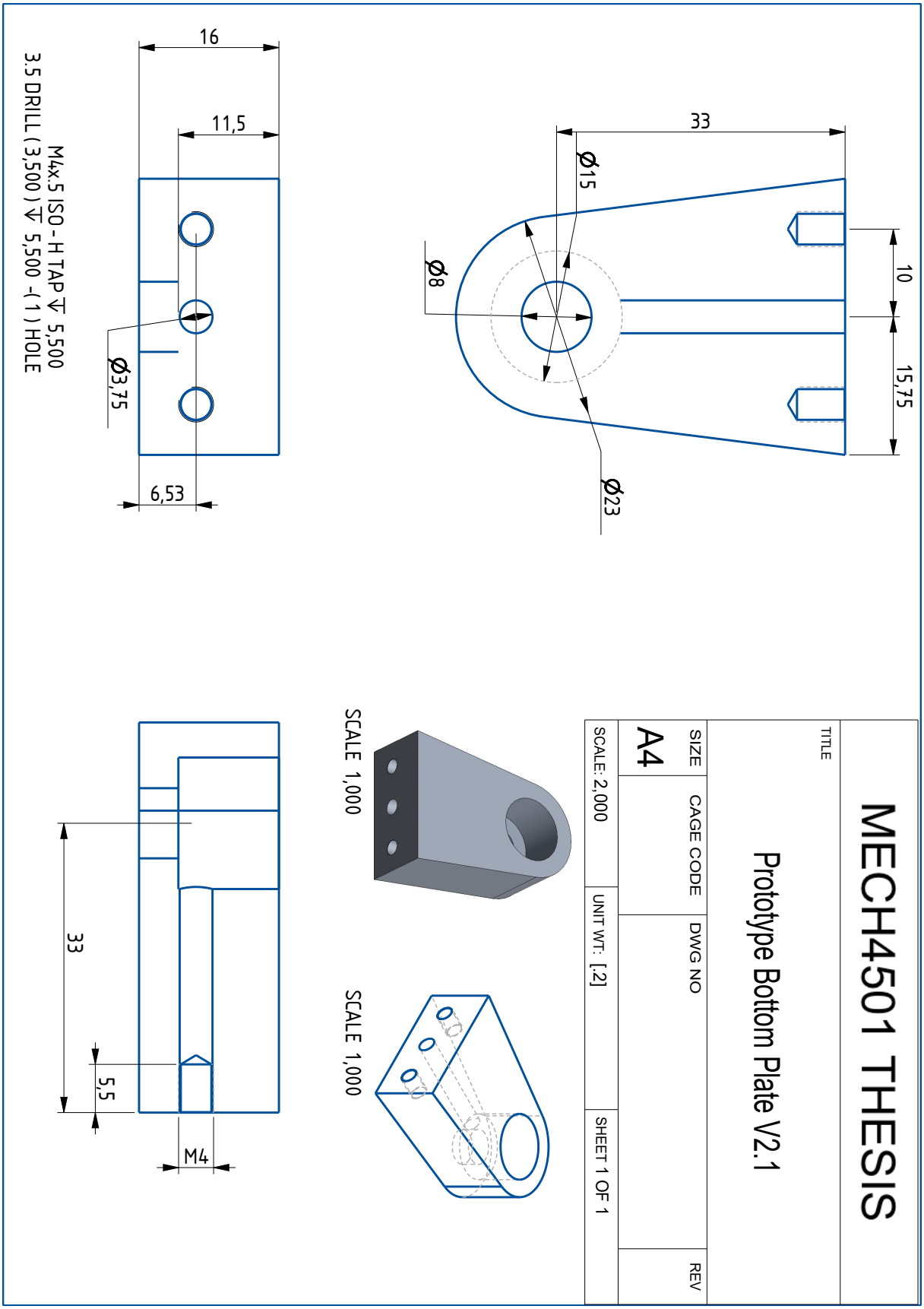

Appendix G – Installation Guide

The following guide should be used in conjunction with manufacturer service manuals for the fork used with the bottom-out damper.

INSTALLING THE BOTTOM-OUT-DAMPER

1. Remove the suspension fork lowers as per manufacturer instructions. For air sprung forks, remove all air pressure using a shock pump.

2. Slide the piston onto the rebound damper rod on the right-hand side. Push it down until it is seated against the stanchion as shown.

3. Re-install the fork lowers, tightening only the bottom bolt on the air side with a 5 mm hex driver (left-hand side). Ensure the rebound damper rod is centred on the bolt in the lowers for the right hand side, where the piston was installed.

4. Place the rubber washer over the bottom bolt hole and install the bottom-out damper as shown by tightening the bolt provided with a 6 mm hex driver. Do not overtighten the bottom bolt.

5. Push the top cap on the reservoir down into the damper body and remove the retaining ring.

6. Remove the top cap using a 1.5 or 2 mm hex driver.

7. Remove the bleed port screw from the internal floating piston using a 2 mm hex driver.

8. Inject 60 mL of Castrol 10Wt Suspension fluid into the damper using a syringe. Push the fork down until fluid passes back into the syringe to bleed the system. Remove the Syringe and reinstall the bleed port screw.

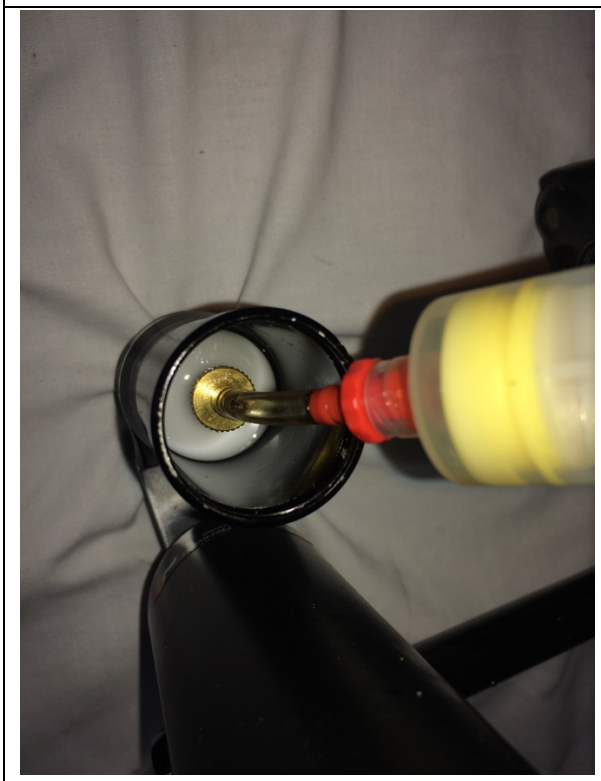

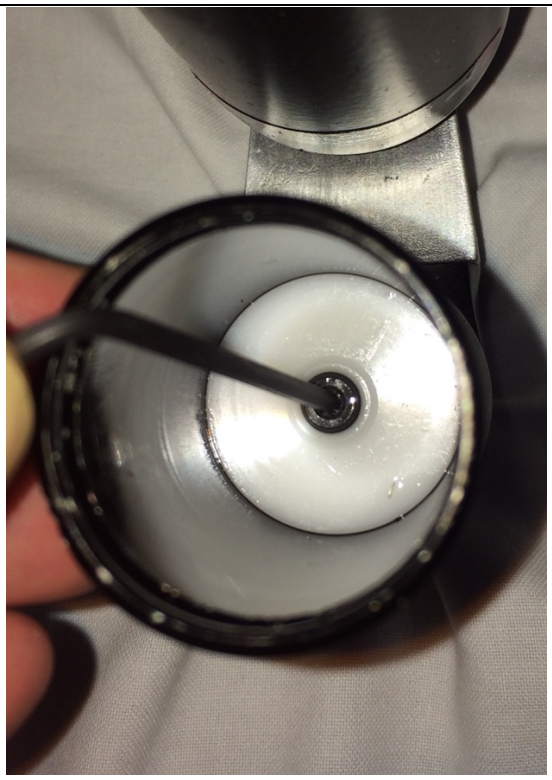

9. Reinstall the top cap and retaining ring as for steps 5 and 6. Using a Rockshox IFP valve adapter tool and shock pump, inflate the IFP chamber to 20-30 psi. Screw on the the IFP valve cap.

10. For air sprung forks, inflate the air spring to the desired pressure. Reinstall the wheel and brake as per manufacturer's instructions. You are ready to RIDE.

Appendix H – Design Specifications

Rockshox Super Deluxe Rear Shock Product Information

Product information about the Rockshox shock that uses the external reservoir component employed in the bottom out damper design can be found at:
https://www.sram.com/rockshox/products/super-deluxe-coil-rct

The service manual for the shock is available online at:
https://sram-cdn-pull-zone-gsdesign.netdna-ssl.com/cdn/farfuture/MVXP_jf3P5RwQrulthVtYQaGN6XoJvTDxHc836-oTRA/mtime:1527202305/sites/default/files/techdocs/gen0000000005361_rev_b_2018_super_deluxe_coil.pdf

Pages 22-28 provide information relevant to servicing the reservoir employed in the bottom out damper design.

Bottom Plate Geometry Report

Volume	8.98 cm^3
Surface Area	4.64 cm^2
Density	2.71 kg/m^3
Mass	24.3 g

Bolts and Washers

Name	Size	Notes
Bottom Bolt	M8x1.0 ISO 27 mm	Allen head (hex), 2.5 mm hollow drilled.
Reservoir Bolts (x2)	M4x0.5 ISO 5.5 mm	Allen head (hex), fine thread.
Rubber washer	15/20 mm (internal/external)	Fits between fork and bottom plate.
Nylon washer	8/10 mm (internal/external)	Fits on bottom bolt below bottom plate.

Component Mass

Component	Mass (g)
Shock Reservoir	102
Bottom Plate	25
Piston	15
Bottom Bolt	18
Spacer	16
Other parts	12
Total	**188**
Suspension Oil	**55**

Evidence of combined weight

Castrol 10 Wt Suspension Fluid Properties

Typical Characteristics

Name	Method	Units	Castrol Fork Oil 10W
Density @ 15C, Relative	ASTM D1298	g/ml	0.88
Viscosity, Kinematic 40C	ASTM D445	mm²/s	15
Viscosity Index	ASTM D2270	None	151
Pour Point	ASTM D97	°C	-48
Flash Point, PMCC	ASTM D93	°C	160
Viscosity, Kinematic 100C	ASTM D445	mm²/s	3.8

Product Data Sheet:
https://msdspds.castrol.com/bpglis/FusionPDS.nsf/Files/210EFB79999B916880257B8A0050C0FD/$File/BPXE-98RJMS.pdf

Appendix I – Validation Results

Standard Fork – Case 1

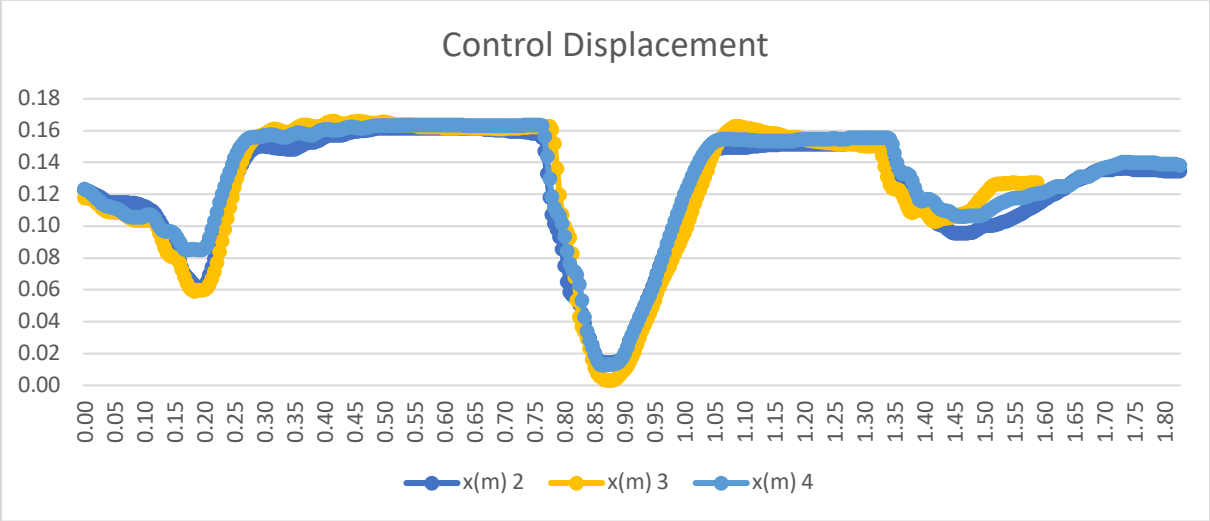

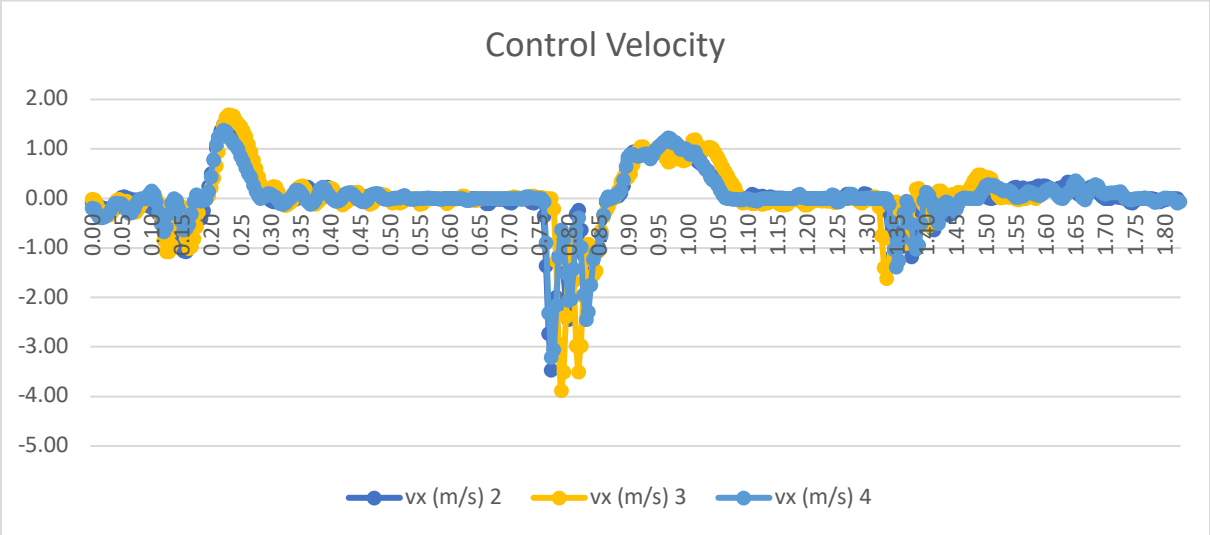

Bottom-Out Open – Case 2

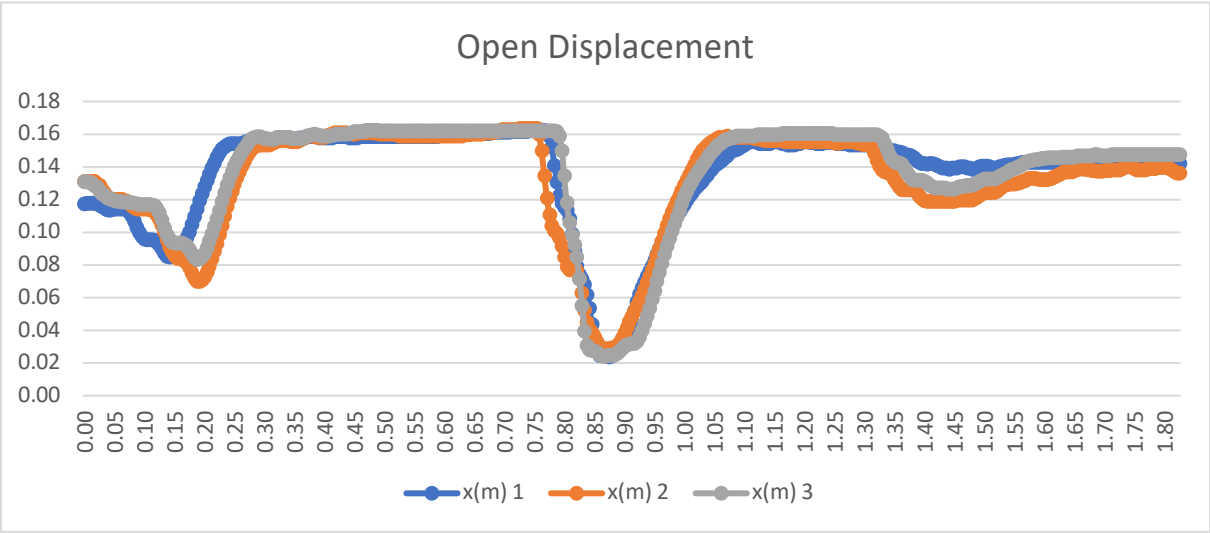

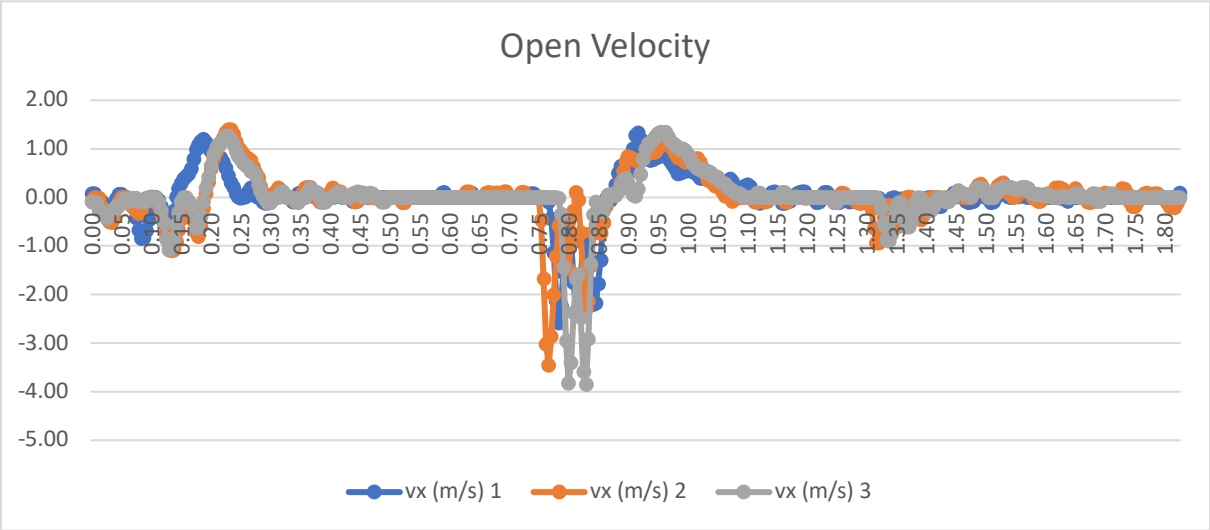

Bottom-Out Quarter – Case 3

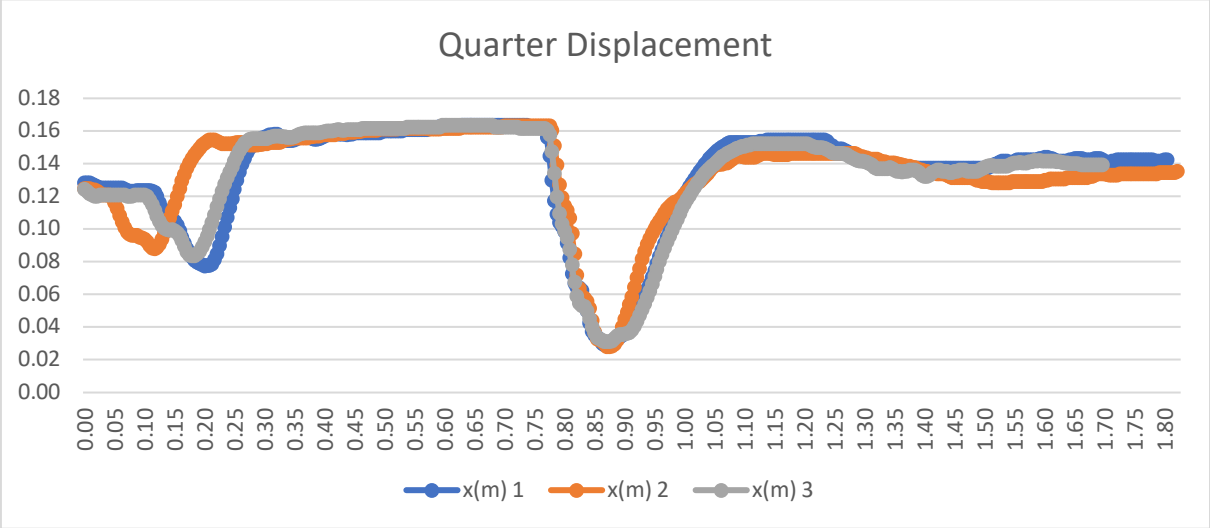

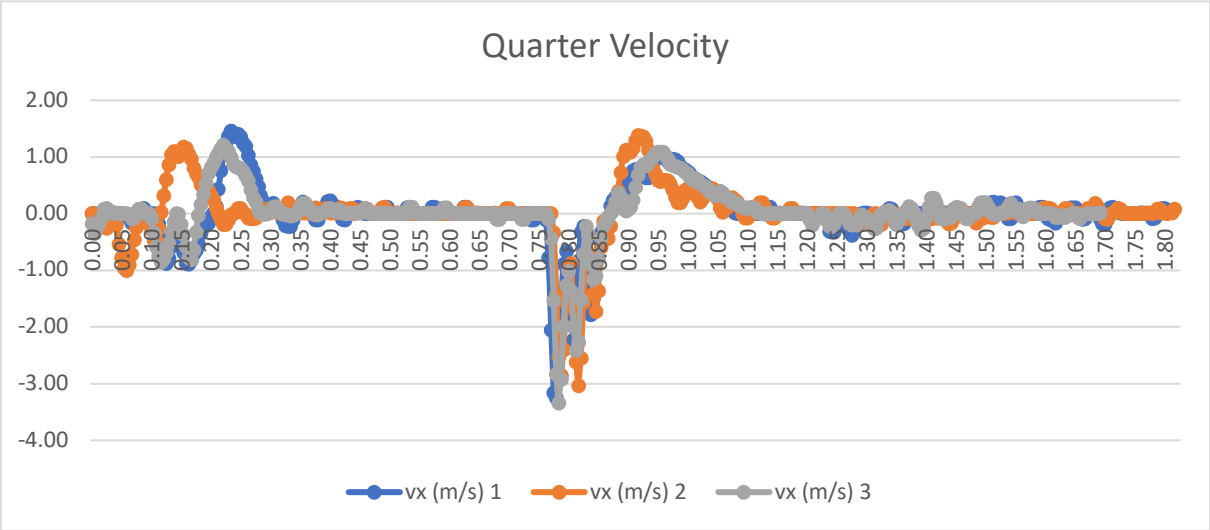

Bottom-Out Half – Case 4

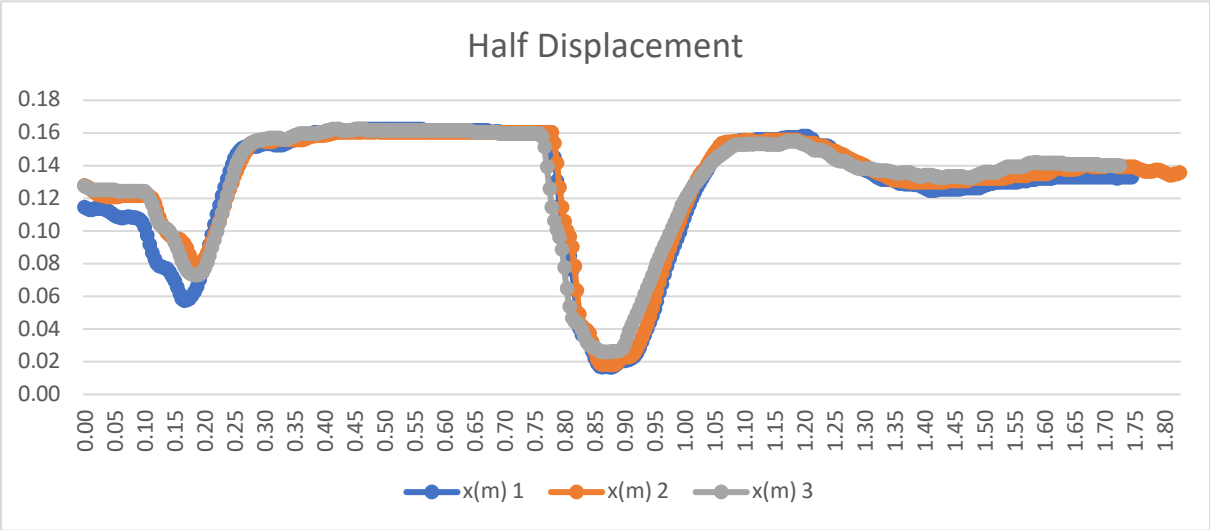

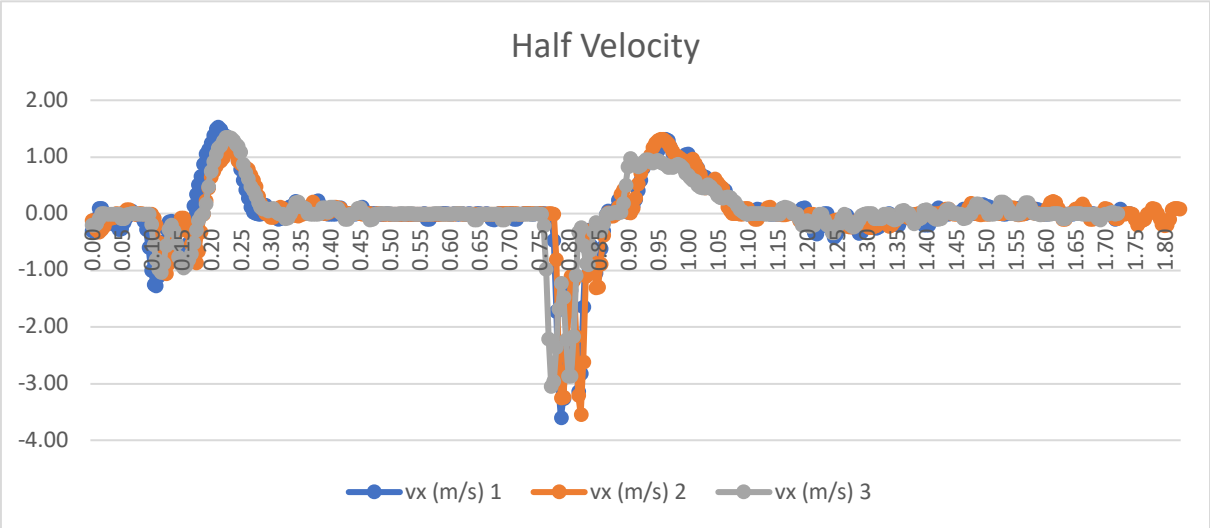

Bottom Out Threequarter – Case 5

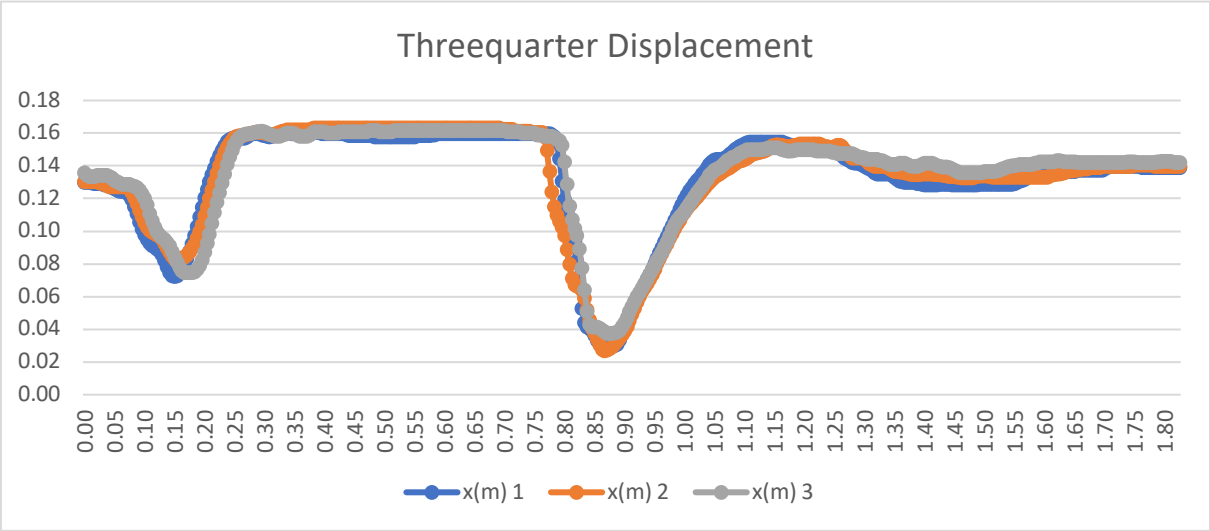

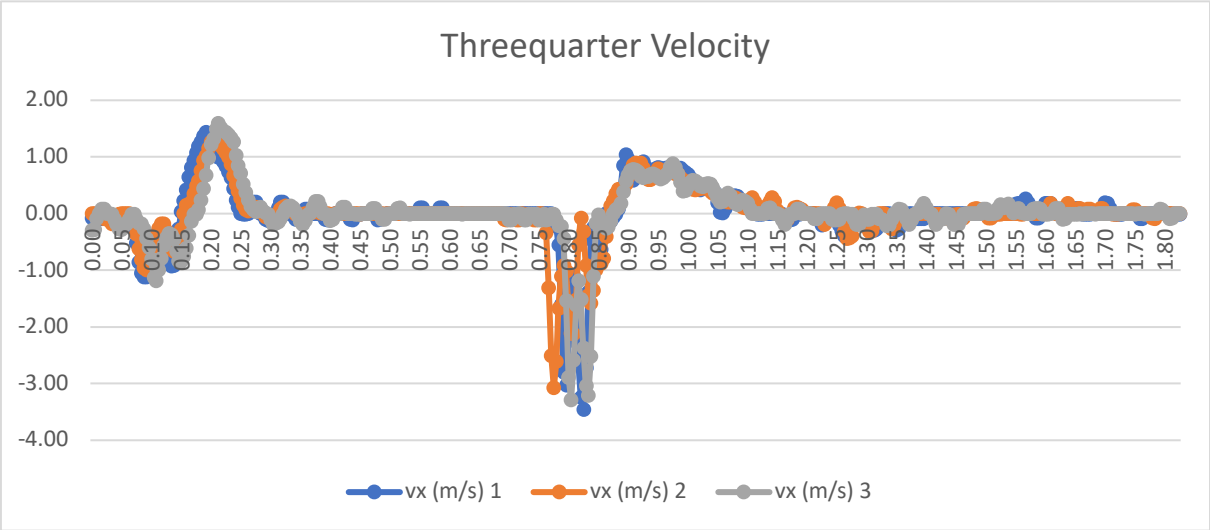

Bottom-Out Closed – Case 6